

# A Global Database of Marine Isotope Substage 5a and 5c Marine Terraces and Paleoshoreline Indicators

Schmitty B. Thompson<sup>1</sup> and Jessica R. Creveling<sup>1</sup>

<sup>1</sup>College of Earth, Ocean, and Atmospheric Sciences, Oregon State University, Corvallis, OR, USA, 97331

Correspondence to: Schmitty B. Thompson (thomschm@oregonstate.edu)

**Abstract.** In this review we compile and document the elevation, indicative meaning, and chronology of Marine Isotope Substage 5a and 5c sea level indicators for 39 sites within three geographic regions: the North American Pacific coast, the North American Atlantic coast and the Caribbean, and the remaining globe. These relative sea level indicators, comprised of geomorphic indicators such as marine and coral reef terraces, eolianites, and sedimentary marine and terrestrial limiting facies, facilitate future investigation into Marine Isotope Substage 5a and 5c interstadial paleo-sea level reconstruction, glacial isostatic adjustment, and Quaternary tectonic deformation. The open access database, presented in the format of the World Atlas of Last Interglacial Shorelines (WALIS) database, can be found at <https://doi.org/10.5281/zenodo.4426206> (Thompson and Creveling, 2021).

## 1 Introduction

Two orbitally modulated peaks in northern hemisphere summer insolation, occurring ~100 and ~80 ka, brought warmer temperatures and reduced ice volumes that briefly interrupted earth's transition from the last interglacial into the last glacial maximum (Milankovitch et al., 1938; Hays et al., 1976; Chappell and Shackleton, 1986; Lambeck and Chappell, 2001; Cutler et al., 2003). These interstadials induced  $\delta^{18}\text{O}_{\text{benthic}}$  excursions, designated as Marine Isotope Substages (MIS) 5c and 5a, coincident with highstands in sea level inferred from uplifted reefs and wave-cut platforms and additional sedimentological indicators (Mesolella et al., 1969; Railsback et al., 2015). Inquiry into MIS 5a and 5c sea level highstands enriches our understanding of last interglaciation (*sensu lato*) paleoclimate (e.g., Potter et al., 2004) and tectonic deformation (e.g., Simms et al., 2016), and faunal assemblages preserved on and within marine terraces reveal ocean paleo-temperature and paleo-circulation pathways (Muhs et al., 2012), all of which complement insight gained from the preceding MIS 5e substage (Kopp et al., 2009; Dutton and Lambeck, 2012; Dutton et al., 2015).

A rich literature catalogues the legacy of mapping globally distributed MIS 5a and 5c reef tracts, wave-cut platforms, and other marine- and terrestrial-limiting sedimentological indicators for the purpose of measuring the local peak sea level achieved during these ice-volume minima (Griggs, 1945; Alexander, 1953; Bretz, 1960; Land et al., 1967; Mesolella, 1967; Chappell, 1974; Chappell and Vech, 1978; Cronin et al., 1981). Here we adopt the standardized framework provided by the World Atlas of Last Interglacial Shorelines (WALIS) database (WALIS, <https://warmcoasts.eu/world-atlas.html>) to compile

Deleted: detail

Deleted: Pacific coast of

Deleted: Atlantic coast of

Formatted: Font: Not Italic

Formatted: Font: Not Italic

Formatted: Font: Not Italic

Deleted: high stand

Deleted: terraces

Formatted: Font: Not Italic

Formatted: Font: Not Italic

Deleted: high stand

Formatted: Font: Not Italic

Deleted: terraces

Formatted: Not Highlight

Formatted: Font: Not Italic

Formatted: Font: Not Italic

the English-language publications of globally outcropping relative sea level (RSL) indicators ascribed by the primary authors as MIS 5a and 5c in age. The open-access database, which includes site descriptions, elevation and geochronological constraints, and associated metadata, is available at this link: <https://doi.org/10.5281/zenodo.4426206> (Thompson and Creveling, 2021). Database field descriptors can be queried at this link: <https://doi.org/10.5281/zenodo.3961543> (Rovere et al., 2020). This database builds on foundational regional syntheses of MIS 5a and 5c sea level indicators for the Atlantic coast of North America and the Caribbean (Potter and Lambeck, 2004), Pacific coast of the United States and Baja California, Mexico (Muhs et al., 2012; Simms et al., 2016), and a subset of far-field localities (Creveling et al., 2017) in compiling a global dataset of 39 sites (Figure 1). The database includes site excluded from previous reviews.

The following sections include a summary of the types of geomorphic and sedimentological sea level indicators included in this review (Section 2); details on how elevation measurements, measurement uncertainty, and sea level data are reported (Section 3); and an overview of the dating methods utilized in the primary publications (Section 4). The majority of this publication (Section 5) reports the current measured elevations and chronologies, along with the history of the literature, for individual sites. Section 6 summarizes future research directions. Section 7 addresses the data availability.

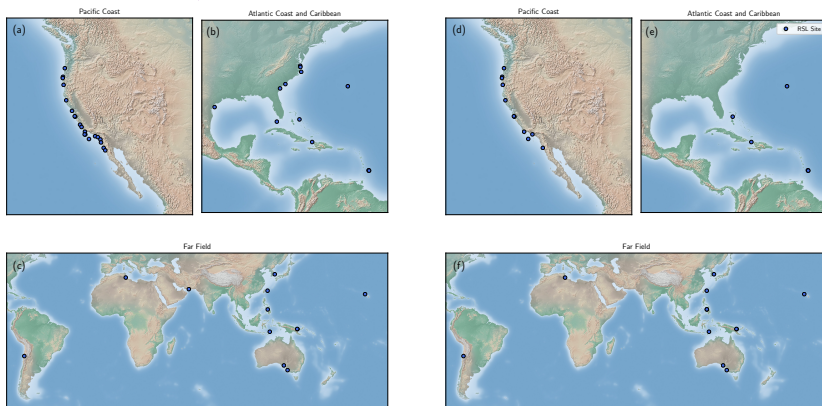


Figure 1: Locations of MIS 5a (a–c) and MIS 5c (d–e) RSL indicator sites for (a,d) the Pacific coast of North America, (b,e) Atlantic coast of North America and the Caribbean, and (c,f) the remaining globe atop the Matplotlib Basemap Shaded Relief map (Hunter, 2007).

The present elevation of MIS 5a and 5c sea level indicators reflects a number of convolved processes, including, but not limited to, tectonic deformation and glacial isostatic adjustment (GIA), which require carefully applied corrections to reconstruct peak global mean sea level (GMSL). Tectonic deformation can alter the elevation of an indicator by tens to hundreds of meters (Alexander, 1953; Chappell, 1974),

Deleted: 3

Deleted: 6

Deleted: with MIS 5a and 5c paleo-sea level indicators

Deleted:

Deleted: the content of this review for

Deleted: relative sea level (

Deleted: )

and glacial isostatic adjustment by similar magnitudes (Creveling et al., 2015; Simms et al., 2016). For active margins, this convolution serves as an opportunity to constrain rates of Quaternary tectonic deformation (Adams, 1984; Marquardt et al., 2004; Muhs et al., 2014) given robust assumptions of the magnitude and source of MIS 5e ice-volume melt and glacial isostatic adjustment (Broecker et al., 1968; Dodge et al., 1983; Chappell and Shackleton, 1986; Creveling et al., 2015; Simms et al., 2016). Similarly after correction for tectonic uplift, discrepancies in the local elevation of globally distributed MIS 5a and 5c indicators of peak sea level retain a meaningful signal of glacial isostatic adjustment (Potter and Lambeck, 2004) which, in turn, allows for the reconstruction of peak global mean sea level and assessments of the sensitivity of Quaternary ice sheets to the influence of Milankovitch forcing on climate in sub-100 kyr timescales (Lambeck and Chappell, 2001; Potter and Lambeck, 2004; Potter et al., 2004; Muhs et al., 2012; Simms et al., 2016; Creveling et al., 2017). We emphasize that this database reports measurements of uncorrected, present-day elevation of various relative sea level indicators that will enable the user to apply corrections based on the most current data- and model-based predictions.

- Formatted: Font: Not Italic
- Formatted: Font: Not Italic
- Formatted: Font: Not Italic
- Formatted: Font: Not Italic
- Formatted: Font: Not Italic
- Formatted: Font: Not Italic
- Formatted: Font: Not Italic
- Deleted: GIA;
- Deleted: 3
- Deleted: 1 (GMSL)
- Deleted: 3
- Formatted: Font: Not Italic
- Formatted: Font: Not Italic
- Formatted: Font: Not Italic
- Formatted: Font: Not Italic
- Deleted: such

## 90 2 Sea Level Indicators

The data detailed in this review (and the associated database) comprises a set of geomorphic and sedimentological indicators of past sea level, for which a comprehensive overview can be found in Rovere et al. (2016). Wave-cut marine platforms make up the largest portion of these data, particularly for the North American Pacific coast (see Muhs et al., 1992b for a detailed description of this indicator). Constructional coral reef terraces are prevalent across North American Atlantic coast, the Caribbean, and the far field regions (see Chappell (1974) for an example of this indicator). Additional sedimentary features, such as eolianites, submerged beach ridges, and exposure surfaces, make up the remainder of the local inferences.

- Formatted: Font: Not Italic
- Deleted: bedrock
- Deleted: terraces
- Deleted: west coast of
- Deleted: the east coast of
- Deleted: When referring to specific sea level indicators, we utilized the terminology used by the primary authors....

## 3 Elevation Measurements

100 Here we catalogue the elevation, with uncertainty (if listed), of a given indicator as reported in the primary publication(s) without modification. Methods adopted to measure the present-day elevation range of reported indicators vary from hand level and altimeter surveys to mapping with modern differential GPS and Digital Elevation Models. The majority of publications summarized herein did not report the sea level datum that the elevation references and, thus, these methods are reported in the  
 105 WALIS database as “Not Reported”. For those sites for which primarily field workers did not report elevation uncertainty, we noted this absence in the database and assigned a measurement uncertainty based upon the defined accuracy of the elevation measurement method. When available in the original publication, latitude and longitude coordinates for indicator sites are reproduced for the WALIS database; when unavailable, coordinates were interpreted from publication maps using Google Earth  
 110 and noted accordingly.

- Deleted: used
- Deleted: General Definition
- Deleted: as defined in the metadata

130 For each site we rated the quality of the RSL elevation data following criteria established by the World  
Atlas of Last Interglacial Shorelines project documentation (see Relative Sea Level at  
<https://doi.org/10.5281/zenodo.3961544>). Quality assessments for RSL elevation reflect a combination  
of measurement precision, the specificity of the reference datum for the elevation, and the range and  
135 uncertainty of the indicative meaning (*sensu* Rovere et al., 2016). When these three variables constrain  
total RSL uncertainty to <1 m or 1–2 m, then WALIS defines the RSL elevation as quality excellent (5)  
or good (4), respectively. If, however, uncertainties in these three variables lead to a RSL elevation of  
2–3 m or > 3m, then a rating of average (3) or poor (2) applies, respectively. For sites without a  
specified reference datum (e.g., 3 m below sea level rather than 3 m below mean high tide), we limited  
140 the maximum quality rating to 3 and assigned a rating based on the remaining factors. Any RSL  
indicator of poorer quality than described above receives a very poor quality rating (1). Any terrestrial  
or marine limiting indicator that serves only as an upper or lower bound on RSL receives a rating of  
rejected (0). Not all primary references report the indicative meaning of an RSL indicator, and thus for a  
subset of sites we calculated the indicative meaning with the IMCalc software (Lorscheid and Rovere,  
2019) in order to assign an elevation quality rating.

Deleted: the precision of the

Deleted: final

Deleted: MHT

Deleted: (i.e., a terrestrial or marine limiting indicator, respectively) receives a rati

#### 4 Dating Techniques

Age assignments for MIS 5a and 5c sea level indicators arise from a wide variety of radiometric and  
non-traditional geochronologic methods. Numeric chronologies for indicators composed of *in situ*  
carbonate utilize uranium-series dating (Barnes et al., 1956; Broecker and Thurber, 1965; Osmond et  
145 al., 1965; Thurber et al., 1965; Muhs et al., 2002; 2012). Sediment mantling sea level indicators can also  
yield numeric chronologies through luminescence dating (Duller, 2004; Grove et al., 2010). Amino acid  
racemization (AAR) creates relative chronologies, especially in conjunction with other amino acid  
ratios from sea level indicators benchmarked by radiometric ages (Mitterer, 1974; Miller et al., 1979;  
Kennedy et al., 1982). Stratigraphic relationships between adjacent sea level indicators have been  
150 extensively used to develop relative chronologies for sea level indicators, especially for sites with  
marine terrace sequences consisting of adjacent MIS 5e, 5c, and 5a terraces (Adams et al., 1984;  
Merritts and Bull, 1989; McInnelly and Kelsey, 1990). Other sparingly used dating methods for MIS 5a  
and 5c indicators include: electron spin resonance (Mirecki et al., 1995), terrestrial cosmogenic nuclide  
dating (Perg et al., 2001), protactinium-231 dating, (Edwards et al., 1997), paleomagnetic stratigraphy  
155 (see sources discussed in Choi et al., 2008), soil development stages (Kelsey et al., 1996), radiocarbon  
dating (Hanson et al., 1992), and geomorphic models (Hanks et al., 1984; Valensise and Ward, 1991).

Deleted: Absolute

Deleted: thorium

Formatted: Font: Not Italic

Formatted: Font: Not Italic

Formatted: Font: Not Italic

Formatted: Font: Not Italic

Deleted: absolute

Formatted: Font: Not Italic

Deleted: dates

Formatted: Font: Not Italic

Formatted: Font: Not Italic

Formatted: Font: Not Italic

Formatted: Font: Not Italic

Formatted: Font: Not Italic

Deleted: Protactinium

Formatted: Font: Not Italic

Formatted: Font: Not Italic

Formatted: Font: Not Italic

Formatted: Font: Not Italic

Formatted: Font: Not Italic

160 For each site we rated the quality of the RSL chronology following criteria established by the World  
Atlas of Last Interglacial Shorelines project documentation (see Relative Sea Level at  
<https://doi.org/10.5281/zenodo.3961544>). Quality assessment of indicator age reflects how well the  
geochronology translates to a stage versus substage assignment. An excellent rating (5) attributes a RSL  
indicator to a narrow window within a substage of MIS 5 whereas a good rating (4) more generally  
assigns an RSL indicator to a substage. If geochronology only assigns an indicator to a generic  
interglacial (such as MIS 5), then this warrants an average rating (3). A poor rating (2) applies to

incomplete chronologic data, or data that provides only a minimum or maximum age on the RSL indicator. Conflicting age assignments between marine isotope stages warrant a very poor quality rating (1). Finally, chronologic data unable to distinguish between two or more Pleistocene Epoch interglacials warrants a rejected quality rating (0).

## 5 A Global Database of Marine Isotope Substage 5a and 5c Relative Sea Level Indicators

### 5.1 North American Pacific Coast

Field observers first documented emergent marine terraces on the North American Pacific Coast in the early 20th century. Early mapping efforts documented terraces along much of the California coastline (Ellis 1919; Davis, 1932; Woodring et al. 1946). Alexander (1953) pioneered the interpretation of west coast marine terraces as indicators of paleo-sea level and tectonic uplift. Since then, extensive documentation of regional MIS 5a and 5c paleo sea level indicators has yielded 18 sites which are included in the present review. As noted below, many such studies reported geomorphic or chronological data that applies to multiple adjacent sites. Griggs (1945) completed early work on the Oregon coast, documenting four terraces, for which we focus on the Whisky Run and Pioneer terraces. McNelly and Kelsey (1990) provided further geomorphic cross sections for the Whisky Run and Pioneer terraces at the Cape Arago and Coquille point sites. Early chronologies for many west coast sites come from Kennedy et al. (1982), which provided <sup>14</sup>C D:L ratios for individual sites plotted against isochrons independently constrained by uranium-series ages. These sites were summarized by Simms et al. (2016), which compared tectonically corrected RSL sites to models of Pacific coast glacial isostatic adjustment.

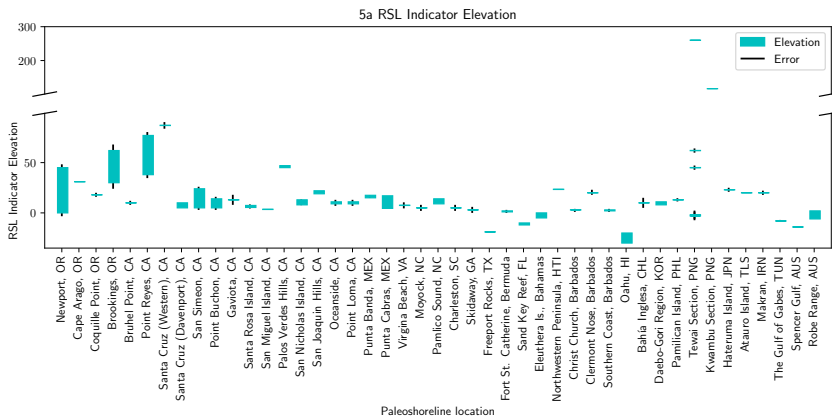


Figure 2: The present elevation of MIS 5a RSL indicators, in meters, at the field locations listed on the horizontal axis. Teal bars represent the full elevation range reported in the primary publications along with the corresponding measurement error, if any, in black bars. Note the scale break on the vertical axis necessary to present indicator elevations for sites with rapid tectonic uplift.

Deleted: bounding age (

Deleted: /

Deleted: )

Deleted: sub

Formatted: English (US)

Formatted: Heading 1

Deleted: ¶

Deleted: West Coast of

Deleted: west coast of

Deleted:

Formatted: Font: Not Italic

Deleted: following

Deleted: Whiskey

Deleted: Whiskey

Deleted: Leucine

Formatted: Font: Not Italic

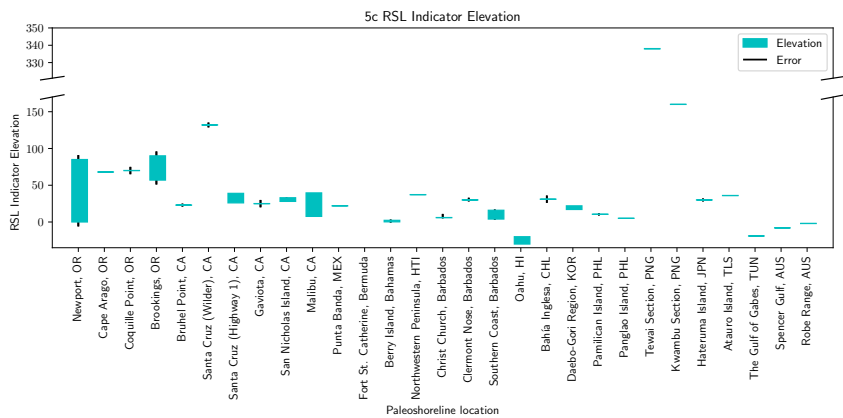
Deleted: dates

Formatted: Font: Not Italic

Deleted: west

Deleted: relative sea level (

Deleted: )



215 **Figure 3: The present elevation of MIS 5c RSL indicators, in meters, at the field locations listed on the horizontal axis. Teal bars represent the full elevation range reported in the primary publications along with the corresponding measurement error, if any, in black bars. Note the scale break on the vertical axis necessary to present indicator elevations for sites with rapid tectonic uplift.**

Deleted: relative sea level (

Deleted: )

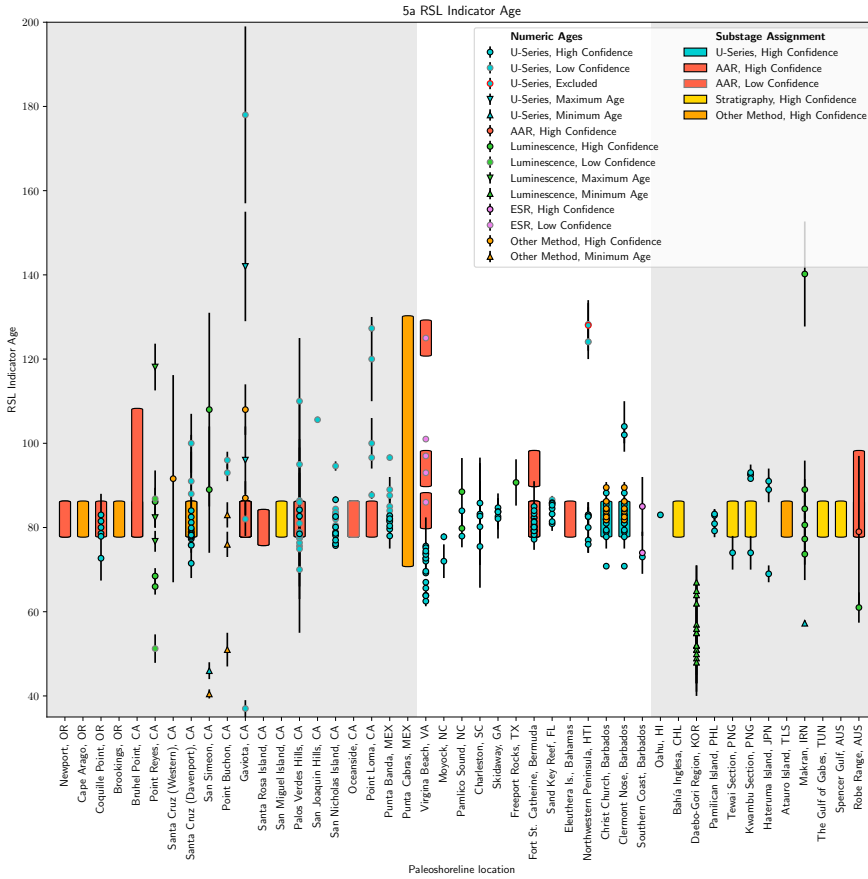
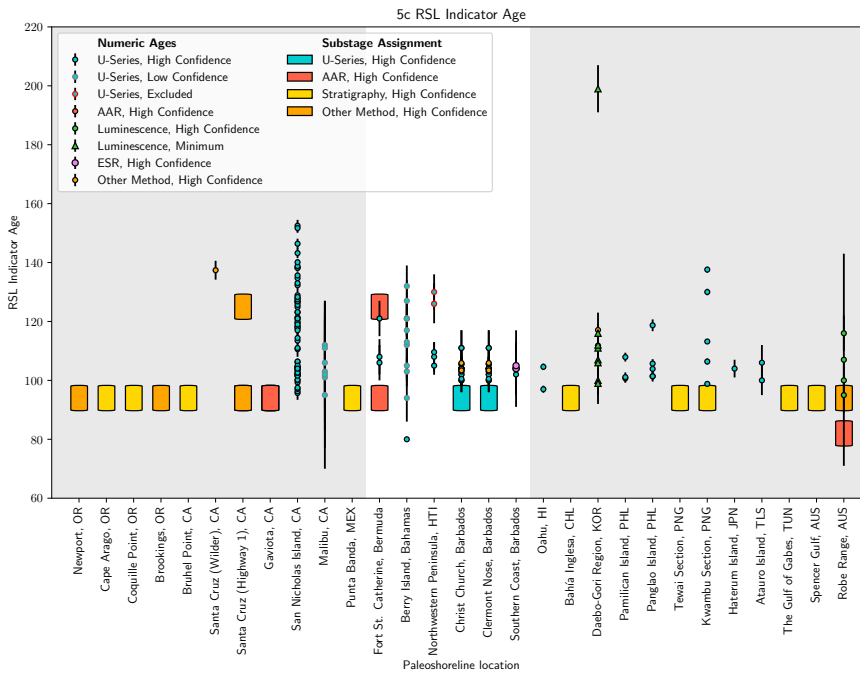


Figure 4: Age assignments for MIS 5a RSL indicators cropping out at the locations listed on the horizontal axis. For each location, the geochronological method is indicated by color, numeric/minimum/maximum age type by shape, and the confidence of the age by border color. Symbols represent numerical ages whereas, in the absence of a numeric chronology, bars represent general Marine Isotope Substage assignments (MIS 5c 98 – 90 ka; MIS 5a 86 – 72 ka).

- Deleted: relative sea level (
- Deleted: )
- Deleted: y
- Deleted: absolute
- Deleted: date
- Deleted: absolute
- Deleted: dates
- Deleted: n
- Deleted: absolute

225



235 Figure 5: Age assignments for MIS 5c RSL indicators cropping out at the locations listed on the horizontal axis. See Figure 4 caption for a description of symbols.

Deleted: relative sea level (  
Deleted: )

### 5.1.1 Newport, Oregon

240 Kelsey et al. (1996) utilized topographic maps and altimeter surveys to map and document the platform elevation ranges of six emergent bedrock terraces which crop out discontinuously through the region due to faulting; we focus on the lowest two of the surveyed platforms, the Newport and Wakonda terraces. Kennedy et al. (1982) first dated the Newport terrace using AAR. The leucine D:L ratio was plotted against isochrons of other AAR ages from proximal locations, assigning the Newport terrace to MIS substage 5a. Kelsey et al. (1996) assigned terraces to MIS substages based on soil development stages. Namely, this study assigned the Newport terrace (0 – 45 m apsl; above present day sea level), which is extensive north of Yaquina Bay and discontinuous between Cape Foulweather and Siletz Bay, to MIS 5a; the Wakonda terrace (0 – 85 m apsl)—which is discontinuous from Newport north to Otter

Formatted: Font: Not Italic

Formatted: Font: Not Italic

Deleted: amino acid racemization (  
Deleted: )

Deleted: Leucine

Deleted: dates

Formatted: Font: Not Italic



255 Rock, and then crops out just above modern beach elevation between Yaquina and Alsea bays before  
gradually descending below sea level south of Alsea Bay—was assigned to MIS 5c. Based on these age  
assignments, Kelsey et al. (1996) correlated the Newport and Wakonda terraces to the Whisky Run and  
Pioneer terraces (see 5.1.2 Cape Arago). Figures 2 and 3 include the terrace elevations reported by  
Kelsey et al. (1996) and Figures 4 and 5 illustrate the MIS substage assignments for the Newport and  
260 Wakonda terraces, respectively (Kennedy et al., 1982; Kelsey et al., 1996).

### 5.1.2 Cape Arago, Oregon

Griggs (1945) mapped four emergent wave-cut platforms along the central Oregon coastline for which  
we focus on the lowest two, the Pioneer and Whisky Run terraces. Adams (1984) documented landward  
tilting of the Pioneer and Whisky Run terraces and the faults that vertically displace them. No  
265 radiometric ages directly constrain the Pioneer and Whisky run terrace chronology at Cape Arago;  
instead, these terraces are assigned to MIS 5a and MIS 5c based on correlation to terraces cropping out  
at Coquille Point (see section 5.1.3; Figures 4 and 5). McNelly and Kelsey (1990) published altimeter  
surveys that revised the peak shoreline angle elevations of the Whisky Run and Pioneer terraces  
reported by Adams (1984) to 31 m apsl and 68 m apsl, respectively (Figures 2 and 3). McNelly and  
270 Kelsey (1990) also reported the thickness of the sediment packages overlying both terraces and revised  
the mapped faults that displace each terrace.

### 5.1.3 Coquille Point, Oregon

This entry focuses on the Pioneer and Whisky Run terraces documented in Griggs (1945). Attribution of  
the Whisky Run terrace to the MIS 5a substage first appeared in Kennedy et al. (1982) based on Leucine  
275 D:L ratios on *Saxidomus* and a single uranium-series age on a coral (Fig. 4). Subsequently, six uranium-  
series ages on corals and bryozoans, 10 amino acid ratios on bivalve mollusks *Mya truncata* and  
*Saxidomus giganteus*, and oxygen isotope stratigraphy on mollusk shells supported the MIS 5a age  
assignment for the Whisky Run terrace (Kennedy et al., 1982; Muhs et al., 1990; Muhs et al., 2006; Fig.  
4). McNelly and Kelsey (1990) revisited the region and presented a representative geomorphic cross-  
280 section that documented deformation of the Whisky Run terrace by the Pioneer anticline. This survey  
reported a Whisky Run terrace maximum elevation of 18 m apsl (Figure 2), a small upward revision  
from the 17 m apsl reported by Muhs et al. (1990). No elevation for the Pioneer terrace was reported in  
the text of this article, though Simms et al. (2016) extracted an elevation of 70 m apsl from the cross-  
section of McNelly and Kelsey (1990). Based on their similar elevations, McNelly and Kelsey (1990)  
285 correlated the Pioneer terrace at Coquille Point with the MIS 5c Pioneer terrace at Cape Blanco, itself  
dated through amino acid ratios and faunal assemblages (Muhs et al., 1990; Figure 5).

### 5.1.4 Brookings, Oregon

Kelsey and Bockheim (1994) utilized topographic maps to document seven wave-cut platforms; the  
lowest two terraces, Harris Butte and Brookings, crop out at bedrock platform elevations of 30 – 62 m  
290 apsl and 57 – 90 m apsl (see Figures 2 and 3), respectively, south of the Whaleshead fault zone. No  
radiometric ages constrain the age of the Harris Butte and Brookings terraces. These terraces were

Formatted: Font: Not Italic

Deleted: Whiskey

Deleted: below

Formatted: Font: Not Italic

Formatted: Font: Not Italic

Formatted: Font: Not Italic

Deleted: terraces

Formatted: Not Highlight

Deleted: dates

Deleted: age of the

Deleted: s

Deleted: below

Deleted: Griggs (1945) mapped four emergent, wave-cut terraces along the central Oregon coastline for which we focus on the lowest two, the  
This entry focuses on the

Formatted: Font: Not Italic

Deleted: who reported

Deleted: Leucine

Deleted: date

Deleted: dates

Deleted: Whiskey

Formatted: Font: Not Italic

Formatted: Font: Not Italic

Formatted: Font: Not Italic

Formatted: Font: Not Italic

Formatted: Font: Not Italic

Deleted: to

Formatted: Font: Not Italic

Deleted: terraces

Formatted: Not Highlight

Deleted: dates

310 assigned to MIS 5a and 5c, respectively, based upon similar soil development stages to the Whisky Run and Pioneer terraces at Cape Arago (Figures 4 and 5).

### 5.1.5 Bruhel Point, California

315 Merritts and Bull (1989) surveyed the 14 marine terraces cropping out at Bruhel Point, for which the 10 m apsl and 23 m apsl terraces (surveyed from the inner edge of the terrace) have been assigned to the MIS 5a and 5c highstands (Figures 2 and 3). A leucine D:L ratio on the 10 m apsl terrace indicates either an MIS 5a or 5c substage designation (Kennedy et al., 1982). In contrast, Merritts and Bull (1989) supported age assignments of MIS 5a and 5c for the 10 m apsl and 23 m apsl terraces, respectively (see Figures 4 and 5), based upon correlations made using diagrams of inferred uplift of the Bruhel Point terraces versus inferred ages (uplift-rate diagrams) to the New Guinea sea level curve (see Section 5.3.6 Tawai and Kwambu).

### 5.1.6 Point Reyes, California

325 Grove et al. (2010) utilized differential GPS to map nine marine terraces across five transects for which the inner edge of the lowest terrace, of purported MIS 5a, was surveyed between 38–77 m apsl (Figure 2). Five sediment samples overlying the lowest terrace yielded three ages per sample from three energy stimuli: optically stimulated blue-light luminescence (OSL), optically stimulated infra-red luminescence (IRSL), and thermoluminescence (TL). Grove et al. (2010) discounted the OSL ages as being too young (MIS 2–3) whereas these authors interpreted TL ages as maximum ages; the IRSL ages were identified as the most accurate estimates of the time of deposition. The sample identified as the best indicator of terrace age (PR-2) assigns the lowest terrace to MIS 5a; the other four samples yield ages ranging from 330 MIS 3 to MIS 5a or show internal inconsistencies (Figure 4).

### 5.1.7 Santa Cruz, California

Alexander (1953) first mapped the emergent marine terraces cropping out in the Santa Cruz, CA region, for which we focus on (often conflicting) interpretations for the age of the laterally extensive, sediment mantled terrace formerly named the Santa Cruz terrace, as well as the two higher elevation Western and 335 Wilder terraces later documented by Bradley and Griggs (1976). Bradley and Addicott (1968) presented four uranium-series ages on mollusks that assigned an age to the Santa Cruz terrace—referred to as the “first” terrace in their nomenclature—consistent with either MIS 5a or 5c. Bradley and Griggs (1976) utilized seismic surveys to subdivide the Santa Cruz terrace into three constituent terraces which, in ascending elevation order include: the Davenport, Highway 1, and Greyhound terraces. A rich literature 340 discusses the chronostratigraphic assignment of the Davenport and Highway 1 terraces. Most authors have concluded, on the basis of amino acid ratios, diffusion modeling of paleo-sea cliffs, and 15 U-series ages on corals, that the Davenport terrace, which crops out at 5 - 10 m apsl (see Muhs et al., 2006), formed during MIS 5a (Kennedy et al., 1982; Hanks et al., 1984; Muhs et al., 2006). The Highway 1 terrace, at an inner edge elevation of 26 – 39 m apsl (Bradley and Griggs, 1976), has been 345 alternately assigned to MIS 5c using models of the diffusion of paleo-sea cliffs (Hanks et al., 1984) or to MIS 5e based upon a geologic fault modeling (Valensise and Ward 1991). In contrast to the above

Deleted: high stand

Deleted: Leucine

Deleted: respectively

Formatted: Font: Not Italic

Deleted:

Deleted: assigned the 10 m apsl and 23 m apsl terraces to

Deleted: ,

Deleted: sections

Formatted: Font: Not Italic

Deleted: dates

Formatted: Font: Not Italic

Deleted: primarily

Deleted: dates

Deleted: for

Deleted: dates

Deleted: were interpreted

Deleted: dates

Deleted: dates

Deleted: dates

Formatted: Font: Not Italic

Formatted: Font: Not Italic

Formatted: Font: Not Italic

Formatted: Font: Not Italic

Deleted: ~26

Formatted: Font: Not Italic

365 chronology, Perg et al. (2001) presented 10 cosmogenic nuclide **ages** that assigned the Santa Cruz  
370 (undifferentiated), Western (87 m apsl; Figure 2), and Wilder (132 m apsl; Figure 3) terraces to MIS 3,  
5a, and 5c respectively. Muhs et al. (2006) contested these cosmogenic **ages**, arguing that they date the  
deposition of alluvium overlying the terraces and therefore provide a minimum age for terrace  
formation. We report Davenport/Highway 1 and Western/Wilder terrace elevations and chronologies as  
separate entries in the database (see Figures 2 – 5) to most accurately represent the existing body of  
literature. For each terrace all of the reported **numeric ages** and age assignments are represented, even  
when conflicting.

Formatted: Font: Not Italic

Deleted: dates

Deleted: dates

Formatted: Font: Not Italic

Deleted: in the database

Deleted: dates

#### 5.1.8 San Simeon, California

375 Hanson et al. (1992) mapped five wave-cut **platforms** along the San Simeon fault zone. North and south  
of the fault zone the San Simeon terrace shoreline angle crops out discontinuously between 5 – 7 m apsl  
and 9 – 24 m apsl, respectively (Figure 2). While a uranium-series **age** on bone and a radiocarbon **age**  
on detrital charcoal provide a minimum terrace age of MIS 3 (Hanson et al., 1992), two  
thermoluminescence **ages** on sediment underlying the emergent platform place the San Simeon terrace  
within the range of MIS 5a to 5c (Berger and Hanson, 1992). Of these possibilities, Simms et al. (2016)  
elected for the MIS 5a San Simeon terrace age assignment (Figure 4).

Deleted: terraces

Formatted: Font: Not Italic

Deleted: dates

Deleted: s

Deleted: date

Formatted: Font: Not Italic

Deleted: dates

Formatted: Font: Not Italic

#### 380 5.1.9 Point Buchon, California

385 Hanson et al. (1992) mapped a flight of marine terraces across south-central California; the lowest  
terrace, Q1, with surveyed shoreline angles between 5 – 14 m apsl, is overlain by up to 2 m of marine  
sediment and 15 – 30 m of non-marine sediment and is cut by several reverse faults (Figure 2). The Q1  
terrace was assigned to MIS 5a based upon three uranium-series **minimum ages** on marine and  
terrestrial mammal teeth and bones found in the overlying sediment deposits (Figure 4). **We included in  
the WALIS database two uranium-series ages on corals considered unreliable by the authors.**

Formatted: Font: Not Italic

Deleted: minimum ages from

Deleted:

Deleted: dates

Deleted: Two

Deleted:

Deleted: dates

Deleted: are included which were noted to be

Deleted: terraces

Deleted: terrace

Deleted: dates

Deleted: .

#### 5.1.10 Gaviota, California

390 Rockwell et al. (1992) mapped five well-expressed marine **abrasion platforms** using transit-stadia  
surveys; the lowest **instance**, the Cojo terrace (10 – 17 m apsl shoreline angle; Figure 2), is found west  
of the South Branch Santa Ynez fault (SBSYF) and crosses the hinge of the Government Point  
Syncline. Seven uranium-series **ages** on bone and mollusk (two of which are maximum ages), eight  
amino acid ratios, and the cool-water aspect of the terrace fauna assign the Cojo terrace to MIS 5a  
(Rockwell et al., 1992; Kennedy et al., 1992; Figure 4). Rockwell et al. (1992) correlated the first  
emergent terrace east of the SBSYF to the Cojo terrace based upon similar amino acid ratios and terrace  
395 faunal aspect. While the elevation of the overlying second terrace at this locale was not reported by  
Rockwell et al. (1992), Simms et al. (2016) extracted an elevation of 25 m apsl from an illustration of  
the shore-parallel terrace profile (see Fig. 2 of Rockwell et al., 1992; Figure 3). No radiometric **ages**  
exist for the second terrace; Rockwell et al. (1992) inferred an MIS 5c age for the second terrace using  
stratigraphic correlation to the 5a terrace and the cool-water aspect of the terrace fauna (Figure 5).

Deleted: dates

### 5.1.11 California Channel Islands (San Miguel and Santa Rosa islands)

Orr (1960) first mapped marine terraces on northwestern Santa Rosa Island and later efforts by Dibble and Ehrenspeck (1998) and Pinter et al. (2001) elaborated on both terrace mapping and the geology of the island. Muhs et al. (2014) utilized differential GPS to map the flight of emergent marine terraces on San Miguel and Santa Rosa Island, for which we focus on the lowest terrace at Santa Rosa Island, with a shoreline angle mapped between 5.4 – 7.4 m apsl, and the lowest terrace at San Miguel Island, with a shoreline angle mapped at ~3.5 m apsl (Figure 2). Two amino acid ratios on *Chlorostoma* shells assigned the lowest Santa Rosa Terrace terrace to MIS 5a (Figure 4). The lowest San Miguel terrace is overlain by a veneer of fossiliferous, cemented gravel and marine sand, which itself is overlain in areas by alluvium (Johnson, 1969; Muhs et al., 2014). Based on stratigraphic position, Muhs et al. (2014) assigned the San Miguel terrace to MIS 5a (Figure 4).

Formatted: Font: Not Italic

Formatted: Font: Not Italic

Deleted: .

Formatted: Font: Not Italic

Formatted: Font: Not Italic

### 5.1.12 Palos Verdes Hills, California

Woodring et al. (1946) conducted early mapping of the 13 emergent, wave-cut platforms of the Palos Verdes Peninsula; seven early uranium-series ages, each corrected for open-system behavior, assigned the first (lowest) terrace to MIS 5a (Szabo and Rosholt 1969). Muhs et al. (1992a) showed, on the basis of aminostratigraphy on *Tegula* and *Protothaca*, and oxygen isotope data on *Epilucina*, that the 'first terrace', as mapped by Woodring et al. (1946), instead represents highstand deposits of both MIS 5a and 5e. Muhs et al. (2006) refined map units and assigned place-based names to supplant the counting scheme of Woodring et al. (1946), redefining the lowest, horizontally continuous surface as the Paseo del Mar terrace (the 'second' terrace of Woodring et al., 1946) with an estimated shoreline elevation angle of ~45 – 47 m apsl (Figure 2). A combination of 13 uranium-series ages on *Balanophyllia* and extralimital northern species within the faunal assemblage assigns the Paseo del Mar terrace to MIS 5a (Figure 4). Around Lunada Bay, Muhs et al. (2006) estimated a ~60–70 m apsl elevation shoreline angle for the 'third' terrace of Woodring et al. (1946), an unnamed intermediate terrace between the Paseo del Mar (MIS 5a) and Gaffey (MIS 5e; the 'fifth' terrace of Woodring et al., 1946); as this terrace does not have geochronological control, we do not include it as MIS 5c indicator.

Formatted: Font: Not Italic

Deleted: terraces

Deleted: dates

Deleted: histories

Formatted: Font: Not Italic

Formatted: Font: Not Italic

Deleted: high stand

Formatted: Font: Not Italic

Formatted: Font: Not Italic

Formatted: Font: Not Italic

Deleted: dates

Deleted: .

Deleted: .

Formatted: Font: Not Italic

Formatted: Font: Not Italic

### 5.1.13 San Joaquin Hills, California

Vedder et al. (1957) first mapped the emergent marine terraces at San Joaquin Hills. Grant et al. (1999) extended the mapping of previous unpublished surveys (see literature discussed therein) and revised the shoreline angle elevation of the first emergent terrace to 19 – 22 m apsl (Figure 2). Based on a single uranium-series age on coral and correlations between terrace height and presumed eustatic sea level, Grant et al. (1999) argued that either the first terrace formed during MIS 5a and hosts reworked MIS 5c coral, or that the MIS 5a and 5c highstands occupied the same terrace (Figure 4).

Formatted: Font: Not Italic

Formatted: Font: Not Italic

Deleted: .

Deleted: date

Deleted: .

Formatted: Font: Not Italic

Deleted: high stand

### 5.1.14 San Nicolas Island, California

Vedder and Norris (1963) mapped 14 emergent bedrock-incised marine terraces on San Nicolas Island and documented their associated faunal assemblages. Muhs et al. (1994; 2006) reported 56 uranium-

Formatted: Font: Not Italic

series [ages](#) on corals found in multiple outcroppings of the lowermost two terraces (terraces 1 and 2) which assign these to MIS 5a and 5e, respectively (Figure 4). Muhs et al. (2012) utilized differential GPS measurements to revise previously reported shoreline angle elevations for terraces 1 and 2 and subdivided terrace 2 into two distinct geomorphic units (terraces 2a and 2b). Muhs et al. (2012) argued that, together, the geomorphic relationships and the 65 new uranium-series [ages](#) on solitary corals supported the conclusions that: (i) terrace 2a (36–38 m apsl) formed during MIS 5e; (ii) terrace 2b (28–33 m apsl), which hosts corals of ~120 and ~100 ka age clusters, formed during MIS 5c and captures reworked fossils from the adjacent, formerly more extensive 5e terrace (terrace 2a); and (iii) terrace 1 (8–13 m apsl) formed during MIS 5a. Muhs et al. (2012) [argued](#) that the distinctive faunal assemblages of terraces 1, 2a and 2b serve to further support their different ages. The terrace elevations reported by Muhs et al. (2012) are shown in Figures 2 and 3; Figures 4 and 5 show the full suite of uranium-series [ages](#) reported for San Nicolas Island terraces 1, 2a, and 2b (Muhs et al., 1994; 2006; 2012). [The MIS 5a and 5c WALIS entries include uranium-series ages MH12-001-001—MH12-055-001 and MH12-057-001 from Chutcharavan and Dutton \(2021\).](#)

- Deleted:** dates
- Formatted:** Font: Not Italic
- Formatted:** Font: Not Italic
- Formatted:** Font: Not Italic
- Deleted:** dates
- Formatted:** Font: Not Italic
- Deleted:** posited
- Formatted:** Font: Not Italic
- Deleted:** dates
- Formatted:** Font: Not Italic
- Deleted:** Chutcharavan and Dutton (2021) entered
- Deleted:** into the WALIS database

#### 5.1.15 Point Loma and Oceanside, California

Ellis (1919) first mapped five marine terraces at Point Loma. Hertlein and Grant (1944) briefly revisited the lower terraces. Carter (1957) extended the mapping to include an additional terrace cropping out lower than the lowest terrace surveyed by Ellis (1919), later named Bird Rock terrace (Kern, 1977). Kern (1973) documented deformation of the Point Loma terraces. Kern and Rockwell (1992) utilized hand levels to revise the shoreline angle elevation of the Bird Rock terrace to 9 – 11 m apsl (Figure 2). The outcropping of Bird Rock terrace to the west at Oceanside is also mapped at 9 – 11 m apsl (Figure 2). Ku and Kern (1974) reported two uranium-series [ages](#) on mollusks but did not utilize these to assign an age to Bird Rock terrace due to secondary uptake of uranium in the mollusk shells. [Uranium-series ages MH02-056-001 derive from Chutcharavan and Dutton \(2021\).](#) In the absence of radiometric [ages](#), calibrated amino acid ratios support a Bird Rock terrace age assignment to MIS 5a (Kern 1977; Kern and Rockwell, 1992; Figure 4).

- Deleted:** dates
- Deleted:** Chutcharavan and Dutton (2021) entered u
- Deleted:** into the WAIS database
- Deleted:** dates

#### 5.1.16 Malibu, California

Davis (1932) mapped three emergent marine terraces around Malibu, California, which, in ascending order, are named the Monic, Dume, and Malibu terraces, for which we focus on the westward tilting Dume terrace. Birkeland (1972) revisited the Dume terrace, of which the shoreline angle sits between ~7 and 40 m apsl (Figure 3). Szabo and Rosholt (1969) reported seven uranium-series [ages](#) on mollusks sampled from the Dume terrace consistent with an MIS 5c age (Figure 5), though these [ages](#) utilized an open-system model to compensate for mobile uranium within shells. If correct, these radiometric ages imply that the Dume terrace correlates with San Nicolas Island terrace 2 (Birkeland 1972; see above). Szabo and Rosholt (1969) and Birkeland (1972) documented a higher, adjacent terrace referred to as terrace C/Corral terrace, which crops out between the Malibu and Dume terraces. Szabo and Rosholt (1969) utilized the same corrected uranium-series methods to assign the Corral terrace to MIS 5e.

- Deleted:** apsl
- Deleted:**
- Deleted:** dates
- Deleted:** dates

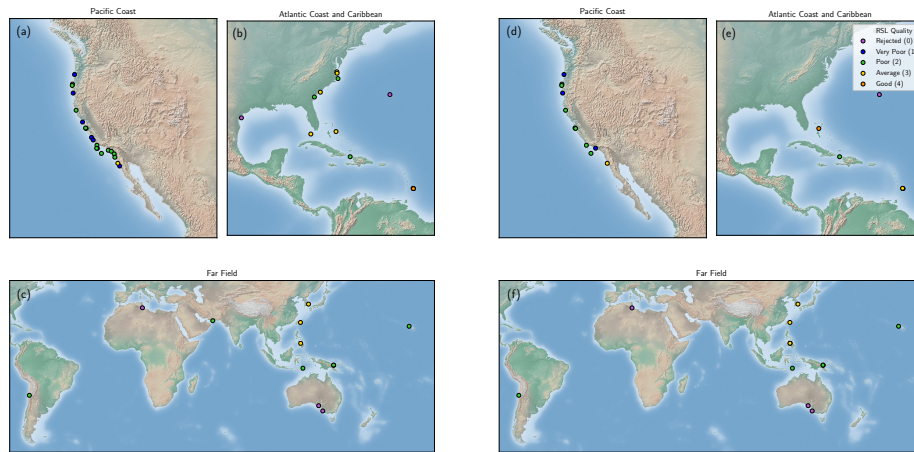
520 5.1.17 Punta Banda, Mexico

Lindgren (1889) first documented Punta Banda marine terraces and Allen et al. (1960) and Rockwell et al. (1989) mapped the lowest 13 and 12 terraces in detail, respectively. The Lighthouse terrace, the lowest mapped terrace (15 – 17.5 m apsl shoreline angle; Figure 2), is well preserved on the south side of the peninsula, though discontinuous on the north side (Rockwell et al., 1989). Fifteen uranium-series ages on *Balanophyllia elegans* assign the Lighthouse terrace to MIS 5a, and extralimital northern species in the faunal assemblage support this designation (Rockwell et al., 1989; Figure 4). A fragmented, narrow second terrace crops out across the Punta Banda peninsula with a shoreline angle of 22 m apsl (Rockwell et al., 1989; Figure 3). No radiometric ages exist for the second terrace, though stratigraphic relationships imply an age of MIS 5c (see discussion in Rockwell et al., 1989; Figure 5).

530 5.1.18 Punta Cabras, Mexico

At Punta Cabras, Baja California, Mexico, Addicott and Emerson (1959) first documented a narrow, discontinuous marine terrace with inner edge elevations of 4.5 – 17 m apsl (Figure 2). No radiometric ages exist for this terrace, though a limited number of radiocarbon ages and extralimital northern species in the faunal assemblage of overlying marine and non-marine deposits support a terrace assignment to MIS 5a (Addicott and Emerson, 1959; Mueller et al., 2009; Figure 4).

535



540 Figure 6. MIS 5a (a-c) and MIS 5c (d-f) sea level indicator elevation quality ratings atop the Matplotlib Basemap Shaded Relief map (Hunter, 2007). For the five Iranian subsites we plotted the lowest quality ratings of those listed in Tables 1 and 2.

**Formatted:** Font: Not Italic

**Formatted:** Font: Not Italic

**Formatted:** Font: Not Italic

**Deleted:** dates

**Formatted:** Font: Not Italic

**Formatted:** Font: Not Italic

**Deleted:** dates

**Deleted:** Muhs et al. (1988) used

**Deleted:** to infer

**Deleted:** dates

**Deleted:** dates

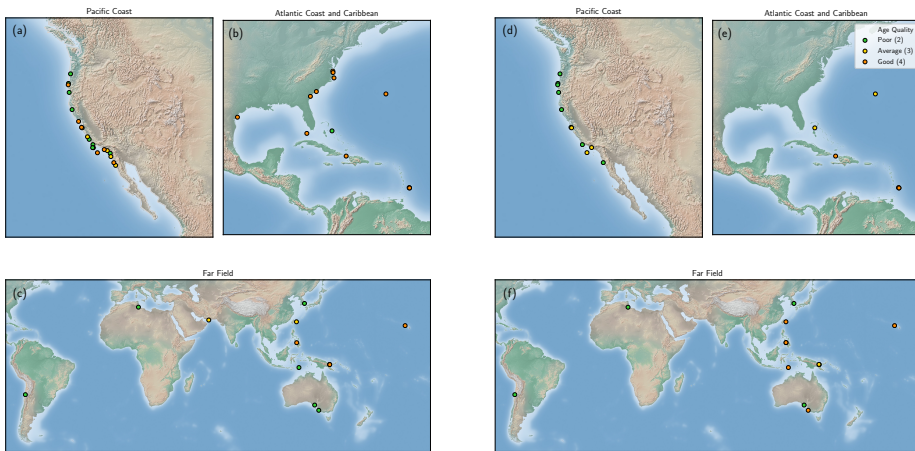


Figure 7. MIS 5a (a-c) and MIS 5c (d-f) sea level indicator chronology quality ratings atop the Matplotlib Basemap Shaded Relief map (Hunter, 2007). For the five Iranian subsites we plotted the lowest quality ratings of those listed in Tables 1 and 2.

### 5.1.19 Summary

Marine terraces comprise the entirety of MIS 5a/5c relative sea level indicators cropping out along the North American Pacific coast. While in principle marine terraces can serve as excellent quality indicators (see 3 and 4), Pacific coast marine terraces receive quality ratings from very poor (1) to average (3) (Figure 6a,d; Tables 1 and 2). These ratings reflect four systematic uncertainties. First, no primary reference reports a terrace's indicative range, the distance between the storm wave swash height and the wave breaking depth (Vacchi et al., 2014; Rovere et al., 2016), and this precludes a calculation of indicative meaning. Given this absence, we used the IMCalc software to quantify the indicative meaning of all Pacific coast marine terraces (WALIS RSL IDs 3473–3503; Lorscheid and Rovere, 2019). The arising indicative ranges tend to vary between 4 and 7.5 m which necessitates quality ratings of poor (2) and lower (as for MIS 5a and 5c terraces at Cape Arago, Coquille Point, Bruhel Point, Gaviota, and San Nicolas Island; MIS 5a terraces at Santa Cruz (Western and Davenport), San Miguel Island, Santa Rosa Island, Oceanside, and Point Loma; and the MIS 5c terrace at Santa Cruz (Wilder)). The MIS 5a and 5c terraces at Punta Banda are the sole exception, as these elevation measurements are sufficiently precise to warrant average quality (3) ratings. Second, the primary literature rarely reports the reference datum for the RSL indicator elevation. Third, the use of altimetry

**Deleted:** The sea level indicators found on the west coast of North American consist primarily of emergent flights of wave-cut marine terraces. Terraces assigned to MIS 5c and 5a are both present at many field localities; a minority of sites include a purported MIS 5c terrace bounded above and below, respectively, by an 5c and 5a terrace. Late Quaternary tectonic deformation affects the majority of west coast terrace exposures (e.g., McInelly and Kelsey), thus all present day terrace elevations must be corrected for tectonics before use in paleo-sea level reconstructions (e.g., Creveling et al., 2015; Simms et al., 2015). Differing vertical displacement across a single field locality complicates this correction and can result in a broad range and terrace elevations with large uncertainties. Overall, MIS 5 substage terraces across this region overall have very good chronologies, particularly those hosting solitary corals suitable for uranium-thorium dating. These radiometric chronologies are supported by the widespread use of calibrated amino acid ratios and stratigraphic relationships. ¶

**Deleted:** (Tables 1 and 2)

**Deleted:** ), Santa Cruz

**Deleted:** (

**Deleted:** is

**Deleted:** is

**Deleted:** an

595 and topographic map measurement techniques before the widespread adoption of differential GPS means that literature-reported measurement uncertainties generally exceed ~3 m (as for the MIS 5a terraces at Palos Verdes Hills and San Joaquin Hills). Fourth, many regional terraces also crop out over a range of elevations due to faulting or tilting, and this range further contributes to RSL uncertainty (such as for MIS 5a and 5c terraces at Newport and Brookings; MIS 5a terraces at Point Reyes, San Simeon, Point Buchon, Punta Cabras; and MIS 5c terraces at Santa Cruz (Highway 1) and Malibu). As all four systematic uncertainties apply to many Pacific coast marine terraces, and at least one uncertainty applies to all terraces, the Pacific coast yields quality ratings of very poor (1) to average (3). From this we conclude that revisiting indicator elevation measurements with modern mapping methods could better constrain Pacific coast MIS 5a and 5c terrace elevations, indicative meanings, and RSL uncertainties.

605 We assigned the chronologies of the North American Pacific coast marine terraces ratings from good (4) to poor (2) (Fig. 7a,d; Tables 1 and 2). The two methods that conferred good quality (4) ratings for this region include: first, reproducible, high precision uranium-series ages on solitary coral skeletal carbonate (as for MIS 5a terraces at Coquille Point, Santa Cruz (Davenport terrace), Palos Verdes Hills, San Nicholas Island, and Punta Banda) and, second, high-precision luminescence ages (as for the MIS 5a Point Reyes marine terrace). For chronologic methods that yielded age uncertainty beyond the bounds of an MIS 5 substage—often arising from substrate experiencing open-system diagenesis—we applied an average (3) quality rating. Examples of this include uranium-series ages on coral (the MIS 5a terrace at San Joaquin Hills and the MIS 5c terrace at Malibu,) or molluscs (the MIS 5a terrace at Point Loma), cosmogenic ages (the MIS 5a and 5c terraces at Santa Cruz (Western and Wilder)), radiocarbon ages (the MIS 5a terrace at Punta Cabras), and luminescence ages (the MIS 5a terrace at San Simeon). While Muhs et al. (2012) interpreted the MIS 5c and 5e uranium-series ages on corals from San Nicholas Island Terrace IIB as an indication of terrace reoccupation, which could afford a good (4) quality rating, here we assign Terrace IIB an average (3) quality rating given that these ages span a time interval longer than either individual MIS substage. Poor quality (2) chronology ratings arise from relative dating methods, such as AAR on molluscs (the MIS 5a and 5c terraces at Gaviota, and the MIS 5a terraces at Newport, Bruhel Point, Santa Rosa Island, and Oceanside), and terrace counting (MIS 5a and 5c terraces at Bruhel Point; the MIS 5a terrace at San Miguel Island; and the MIS 5c terraces at Cape Arago, Coquille Point, and Punta Banda). For this region, chronologic assignment by terrace counting is especially common for MIS 5c terraces with an adjacent, well-dated MIS 5a terrace. Non-traditional methods and maximum/minimum limiting ages confer a poor (2) rating for MIS 5a and 5c terraces at Newport, Brookings, and Gaviota; the MIS 5a terrace at Cape Arago; and the MIS 5c terrace at Santa Cruz (Highway 1 terrace). Likewise, minimum limiting uranium-series age on mammal teeth and bone, and unreliable uranium-series dates on coral (see Hanson et al., 1992) assign Point Buchon a poor quality rating (2). For the North American Pacific coast, MIS 5a terraces generally received higher quality ratings than MIS 5c terraces (Tables 1 and 2).

Deleted: l

Deleted: ,

Deleted: ,

Deleted: ,

Deleted: Importantly,

Deleted: y

Deleted: T

Deleted: a

Deleted: ,

Deleted: )

Deleted: and MIS 5c Santa Cruz (

Deleted: terraces

Deleted: C



645 5.2 North American Atlantic coast and the Caribbean

Deleted: East Coast of

Deleted:

Deleted: &

Deleted: ¶

Formatted: Font: Not Italic

Deleted: east

650 5.2.1 Virginia Beach, Virginia; Moyock, North Carolina; Charleston, South Carolina; and Skidaway, Georgia  
Cronin et al. (1981) mapped emergent coral terraces along the Atlantic coast of the United States, from Virginia to Georgia, and reported reconstructions of paleo-sea level based upon their documented terrace elevations. Wehmiller et al. (2004) revisited the Virginia Beach, Moyock, Charleston and Skidaway sites, and reported the maximum elevation of the four coral bearing units as ~7.5 m apsl, ~5 m apsl, ~5 m apsl and ~3 m apsl respectively (Figure 2). 27 uranium-series ages on corals assign the terraces at these four sites to MIS 5a (Cronin et al., 1981; Szabo, 1985; Wehmiller et al., 2004; see Figure 4). Further, five electron spin resonance ages and eight amino acid ratios at the Virginia Beach site support an age assignment of MIS 5 sensu lato, without a specific substage designation (Mirecki et al., 1995). No MIS 5c-equivalent coral terraces were recognized across this region.

Deleted: ;

Formatted: Font: Not Italic

Deleted:

Deleted: dates

Formatted: Font: Not Italic

Formatted: Font: Not Italic

Deleted: dates

Formatted: Font: Not Italic

Formatted: Font: Not Italic

Formatted: Font: Not Italic

Formatted: Font: Not Italic

Formatted: Font: Not Italic

Formatted: Font: Not Italic

Deleted: further

Deleted: A

Deleted: database

Deleted: of AAR data along

Deleted: from the University of Delaware can be found at Wehmiller (2021b).

Formatted: Font: Not Italic

Formatted: Font: Not Italic

Formatted: Font: Not Italic

Formatted: Font: Not Italic

Formatted: Font: Not Italic

Deleted: date

Formatted: Font: Not Italic

Formatted: Font: Not Italic

Formatted: Font: Not Italic

Formatted: Font: Not Italic

Deleted: dates

Formatted: Font: Not Italic

Formatted: Font: Not Italic

Formatted: Font: Not Italic

Formatted: Font: Not Italic

Formatted: Font: Not Italic

Formatted: Font: Not Italic

Formatted: Font: Not Italic

Formatted: Font: Not Italic

Formatted: Font: Not Italic

Formatted: Font: Not Italic

Formatted: Font: Not Italic

Formatted: Font: Not Italic

Formatted: Font: Not Italic

Formatted: Font: Not Italic

Formatted: Font: Not Italic

Formatted: Font: Not Italic

5.2.2 Pamlico Sound, North Carolina

660 Parham et al. (2013) utilized outcrops and sediment cores to map late Quaternary beach deposits, for which we focus on a deposit primarily composed of a thin veneer of sand and laminated sand. The sequence appears discontinuously through the study site at an elevation of 9 – 14 m apsl (Figure 2): east of the Chowan river, the deposit forms a prograding spit whereas further east of the Suffolk shoreline the deposit forms a seaward thickening wedge, and the deposit is not well preserved in the northern and southern portions of the study area. Shelly marine material within the deposit was assigned to MIS 5a using calibrated amino acid racemization and optically stimulated luminescence dating (Figure 4). Two uranium-series ages now support an MIS 5a age assignment for these beach deposits (Wehmiller et al., 2021a). See Wehmiller (2021b) for a comprehensive database of AAR ages for the North American Atlantic coast.

Deleted: date

Formatted: Font: Not Italic

Formatted: Font: Not Italic

Formatted: Font: Not Italic

Formatted: Font: Not Italic

Formatted: Font: Not Italic

Formatted: Font: Not Italic

Formatted: Font: Not Italic

Formatted: Font: Not Italic

Formatted: Font: Not Italic

Formatted: Font: Not Italic

Formatted: Font: Not Italic

Formatted: Font: Not Italic

Formatted: Font: Not Italic

Formatted: Font: Not Italic

Formatted: Font: Not Italic

Formatted: Font: Not Italic

Formatted: Font: Not Italic

Formatted: Font: Not Italic

Formatted: Font: Not Italic

Formatted: Font: Not Italic

Formatted: Font: Not Italic

5.2.3 Freeport Rocks, Texas

670 Simms et al. (2009) documented a sedimentary deposit within offshore sediment cores, referred to as the Freeport Rocks Bathymetric High, consisting of barrier island facies. The deposit appears at its highest elevation within the core at 18.9 m bpsl (below present day sea level; Figure 2). The authors assign the Freeport Rocks Bathymetric High to MIS 5a based upon a single optically stimulated luminescence age (Figure 4).

Deleted: date

Formatted: Font: Not Italic

Formatted: Font: Not Italic

Formatted: Font: Not Italic

Formatted: Font: Not Italic

Formatted: Font: Not Italic

Formatted: Font: Not Italic

Formatted: Font: Not Italic

Formatted: Font: Not Italic

Formatted: Font: Not Italic

Formatted: Font: Not Italic

Formatted: Font: Not Italic

Formatted: Font: Not Italic

Formatted: Font: Not Italic

Formatted: Font: Not Italic

Formatted: Font: Not Italic

Formatted: Font: Not Italic

Formatted: Font: Not Italic

Formatted: Font: Not Italic

Formatted: Font: Not Italic

Formatted: Font: Not Italic

Formatted: Font: Not Italic

5.2.4 Fort St. Catherine, Bermuda

675 A rich literature describes the evolution of the stratigraphic nomenclature of Bermuda, comprised of six carbonate units separated by terra rosa paleosols (Land et al., 1967; Vacher and Hearty, 1989; Hearty, 2002). The marine member of the Southampton Formation, mapped at 1 m apsl (Vacher and Hearty, 1989), was tentatively assigned to MIS 5a or 5c using amino acid stratigraphy (Harmon et al., 1983; Hearty et al., 1992) though, subsequently, 24 uranium-series ages reported across multiple studies have indicated an MIS 5a age assignment (Harmon et al., 1983; Ludwig et al., 1996; Muhs et al., 2002; see

Deleted: date

Formatted: Font: Not Italic

Formatted: Font: Not Italic

Formatted: Font: Not Italic

Formatted: Font: Not Italic

Formatted: Font: Not Italic

Formatted: Font: Not Italic

Formatted: Font: Not Italic

Formatted: Font: Not Italic

Formatted: Font: Not Italic

Formatted: Font: Not Italic

Formatted: Font: Not Italic

Formatted: Font: Not Italic

Formatted: Font: Not Italic

Formatted: Font: Not Italic

Formatted: Font: Not Italic

Formatted: Font: Not Italic

Formatted: Font: Not Italic

Formatted: Font: Not Italic

Formatted: Font: Not Italic

Formatted: Font: Not Italic

Formatted: Font: Not Italic

700 Figure 4). The Pembroke unit of the Rocky Bay Formation, previously classified as the Pembroke  
Formation (with a proposed alternate name of the Hungry Bay Formation), has generated more debate.  
Amino acid ratios on *Poecilozonites* support a MIS 5c age assignment (Harmon et al., 1983), while  
705 whole rock amino acid ratios support an age assignment of MIS 5e (Hearty et al., 1992). Four uranium-  
series ~~ages~~ yielded one MIS 5e coral, two MIS 5c-aged corals, and one modern coral (Harmon et al.,  
1983; see Figure 5) though Vacher and Hearty (1989) argued that published uranium-series ~~ages~~ were  
unable to resolve an MIS 5 substage for the Rocky Bay Formation, and instead hypothesized that this  
unit represents MIS 5e. For the purposes of this review, the Pembroke unit chronology is included in  
710 ~~Figure 5~~, with both 5c and 5e age assignments included. No elevation was reported for the Pembroke  
unit.

Moreover, controversy exists over the classification of both the Southampton Formation and the  
Pembroke unit of the Rocky Bay Formation. Harmon et al. (1983) hypothesized that both units formed  
715 from storm wave activity and, thus, the deposits do not serve as indicators of a sea level ~~highstand~~.  
Toscano and Lundberg (1999) supported this hypothesis, further specifying that the units were formed  
in the Holocene and incorporated corals of many different ages. Alternatively, other studies argued the  
location of Fort St. Catherine relative to the platform margin and the narrow range of MIS 5a ~~ages~~ on  
720 corals found within the Southampton Formation reveal that these units represent a sea level ~~highstand~~  
(Vacher and Hearty, 1989; Ludwig et al., 1996; Muhs et al., 2002). Here we include both units within  
the database.

#### 5.2.5 Sand Key Reef, Florida

Seismic-reflection profiles documented submerged outlier reefs along the windward side of the modern  
Florida Keys (Lidz et al., 1991; Ludwig et al., 1996; Toscano and Lundberg, 1999). While the Sand Key  
725 Reef shows geomorphic complexity, the primary reef crest sits ~10 – 12 m bpsl (Figure 2). The reef  
primarily comprises *Montastrea annularis*, with a thin overgrowth of reef crest *Acropora palmata*  
(Ludwig et al., 1996). Two radiocarbon ages along with eight uranium-series ~~ages~~ on *Montastrea*  
*annularis*, *Acropora palmata*, and *Colpophyllia natans* assign the main reef growth to MIS 5a (Lidz et  
al., 1991; Ludwig et al., 1996; Toscano and Lundberg, 1999; Figure 4).

#### 725 5.2.6 Eleuthera Island, Bahamas

Skeletal eolianites comprising Eleuthera Island are interpreted as eolian dunes and are separated from  
the underlying formations by paleosols (Kindler and Hearty, 1996; Hearty, 1998; Hearty and Kaufman,  
2000). The authors report an inferred paleo-sea level of 0 – 5 m bpsl, rather the modern elevation of the  
deposit (Hearty and Kaufman, 2000; Figure 2). The stratigraphic position, location, and amount of  
730 diagenetic alteration of the eolianite, along with whole rock amino acid ratios, assign the unit to MIS 5a  
(Figure 4).

#### 5.2.7 Berry Islands, Bahamas

Newell (1965) reported a single uranium-series ~~age~~ for a coral welded with caliche to a platform on  
Berry Island, which assigned the coral to MIS 5a. Neumann and Moore (1975) reported 11 additional

Formatted: Font: Not Italic

Formatted: Font: Not Italic

Deleted: dates

Deleted: -aged

Formatted: Font: Not Italic

Deleted: dates

Deleted: the

Deleted: MIS 5e specific

Deleted: .

Formatted: Font: Not Italic

Deleted: high stand

Deleted: dates

Deleted: high stand

Formatted: Font: Not Italic

Formatted: Font: Not Italic

Formatted: Font: Not Italic

Formatted: Font: Not Italic

Formatted: Font: Not Italic

Deleted: dates

Formatted: Font: Not Italic

Formatted: Font: Not Italic

Deleted: date

uranium-series ages on corals found at 0.2 – 2.3 m apsl (Figure 3) as MIS 5 in age, though the range of ages could not assign the ridge to a specific substage highstand. Creveling et al. (2017) noted that an MIS 5c age assignment for the Berry Islands corals fits the the published age uncertainty (Figure 5).

#### 5.2.8 Northwestern Peninsula, Haiti

750 Woodring et al. (1924) first documented the geology of the Northwestern Peninsula, which was followed by further research summarized by Dodge et al. (1983). Dodge et al. (1983) mapped seven constructional coral reef terraces composed primarily of *Acropora palmata*, for which we focus on the lowest two, the Mole and Saint terraces. Dumas et al. (2006) published altimeter surveys for the Mole and Saint terraces (also referred to as T1 and T2), revising the previously reported inner edge elevations to 23 m apsl and 37 m apsl, respectively (Figures 2 and 3). Dodge et al. (1983) and Dumas et al. (2006) 755 argued that 15 uranium-series ages on corals support the conclusion that: (i) the Mole terrace formed during MIS 5a; (ii) the Saint terrace formed during MIS 5c; (iii) both terraces host corals reworked from the adjacent MIS 5e terrace (see Figures 4 and 5).

#### 5.2.9 Christ Church and Clermont Nose traverses, Southern Coast, Barbados

760 Mesolella (1967) first mapped the coral reef terraces of the Christ Church and Clermont Nose traverses. Bender et al. (1979) revisited nine reef tracts at Christ Church and seven reef tracts at Clermont Nose. 28 uranium-series ages on corals, along with 12 protactinium-231 ages, assign the Worthing and Venter terraces at both traverses to MIS 5a and 5c, respectively (Broecker et al., 1968; Mesolella, 1969; Bender et al., 1979; Bard et al., 1990; Edwards et al., 1997; see Figures 4 and 5). The elevations of the 765 Worthing and Venter terraces are mapped at 3 m apsl and 6 m apsl at Christ Church and 20 m apsl and 30 m apsl at Clermont nose (Figures 2 and 3). Schellmann and Radtke (2004) mapped additional terraces on the south coast. The two sub-terraces T-1a<sub>1</sub> and T-1a<sub>2</sub> were collectively mapped at 2 -3 m apsl and assigned to MIS 5a based on two averaged ESR ages and one uranium-series age (Figures 2 and 4). The sub-terraces T-1b, T-2, and T-3 were collectively mapped at 4 – 16 m apsl and assigned to 770 MIS 5c based on thre averaged ESR ages and one uranium-series age (Figures 3 and 5).

#### 5.2.10 Summary

775 The North American Atlantic coast and Caribbean sea level indicators, which consist of coral reef terraces, beach deposits, and terrestrial limiting beach ridges, received elevation quality ratings from good (4) to rejected (0) (Figure 6b,c; Tables 1 and 2). Since none of the primary literature sources report indicative ranges for the relative sea level indicators along the North Atlantic coast and Caribbean, we calculated these values with the IMCalc software and reported these for WALIS RSL IDs 3504–3508, 3511–3519, 3556, and 3983–3984 (Lorscheid and Rovere, 2019). The clear reference datum for the Berry Island and MIS 5a Christ Church coral reef terraces (Neumann and Moore, 1975; Bender et al., 1979) warrants the only good quality (4) ratings for this region. For MIS 5a and 5c Clermont Nose and those coral reef terraces with no reference data reported (as for MIS 5a RSL indicators at Virginia Beach, Moyock, Charleston, Sand Key Reef, Eleuthera Island, and Southern Coast Barbados), the assigned quality ratings of average (3) reflect the precision of the elevation

Deleted: dates

Deleted: high stand

Deleted: A later review

Formatted: Font: Not Italic

Deleted: samples

Deleted: uncertainty of

Deleted: data

Deleted: Creveling et al., 2017;

Formatted: Font: Not Italic

Formatted: Font: Not Italic

Formatted: Font: Not Italic

Formatted: Font: Not Italic

Formatted: Font: Not Italic

Deleted:

Deleted: dates

Deleted: 3

Deleted: dates

Deleted: Protactinium

Deleted: dates

Formatted: Font: Not Italic

Formatted: Font: Not Italic

Formatted: Font: Not Italic

Deleted:

Deleted: are

Deleted: 2

Deleted: s

Deleted: are

Deleted: 3

Deleted: s

Formatted: Font: 12 pt, Not Bold

Formatted: Font: 12 pt, Not Bold

Formatted: Font: 12 pt, Not Bold

805 measurement reported in the primary literature and indicative ranges equal to, or less than, ~2 m as calculated by IMCalc. Coral reef terraces and beach deposits with a poor quality rating (2) reflect either a greater elevation measurement uncertainty (as for the MIS 5a and 5c RSL indicators at Northwestern Peninsula, the MIS 5a indicator at Pamlico Sound, and the MIS 5c indicators at Christ Church, and Southern Coast Barbados) or an indicative range greater than ~2 as calculated by IMCalc (as for MIS 5a Skidaway). The terrestrial limiting MIS 5a indicator at Freeport Rocks and the MIS 5a and 5c indicators at Fort St. Catherine warrant a rejected (0) quality rating. As with the Pacific coast indicators, we support revisiting coral reef terraces and beach deposit with quality ratings of average (3) to poor (2) to improve uncertainty by applying modern methods for elevation measurement and adopting an updated framework to constrain indicative meaning.

810  
815 We assigned the North American Atlantic Coast and Caribbean chronologies ratings of good (4) to poor (2) (Figures 7b,e; Tables 1 and 2). For this region, good ratings (4) arose from one of two methods: first, high precision uranium-series ages from skeletal coral (from MIS 5a and 5c indicators at Northwestern Peninsula, Christ Church, and Southern Coast; MIS 5a indicators at Virginia Beach, Moyock, Charleston, Skidaway, Sand Key Reef, and Fort St. Catherine; and the MIS 5c indicator at Clermont Nose) and second, high precision luminescence ages (on MIS 5a indicators at Pamlico Sound and Freeport Rocks). Sites that receive an average quality rating (3) have uranium-series based chronologies which span MIS 5 (the MIS 5a indicator at Clermont Nose; and the MIS 5c indicators at Fort St. Catherine and Berry Island). Due to the absence of material available for numerical dating methods at Eleuthera Island, the relative dating methods warrants a quality rating poor (2). We advocate continued focus on sites with average quality ratings (3)—those that have substrate amenable to geochronology yet have imprecise ages—to improve chronologic assignments.

## 825 5.3 Far Field

### 5.3.1 Oahu, Hawaii

830 Sherman et al. (2014) utilized offshore drill cores to document and date two submerged coral reef terraces on Oahu. A single uranium-series age assigned one terrace to MIS 5a; two uranium-series ages assigned a second terrace to MIS 5c (Figures 4 and 5), though distinct elevations were not reported for the MIS 5a and 5c terraces. Instead, a range in elevations from 20 – 30 m bpsl was provided for both terraces (Figures 2 and 3).

### 5.3.2 Bahia Inglesa, Chile

835 Marquardt et al. (2004) utilized altimeter surveys to map eight emergent marine terraces and the overlying fossiliferous terrace deposits. The shoreline angle of the two lowest terraces found above the Holocene beach is mapped at 10 m apsl and 31 m apsl (Figures 2 and 3). Uranium-series and electron spin resonance ages from a neighboring region assign the two terraces to MIS 5, and their stratigraphic position, assuming uniform uplift rate, further assigns the 10 m and 31 m terraces to MIS 5a and 5c (see discussion in Marquardt et al., 2004; Figures 4 and 5).

**Deleted:** (as for MIS 5a Virginia Beach, Moyock, Charleston, Sand Key Reef, Eleuthera Island, Southern Coast). Coral reef

**Formatted:** Font: 12 pt, Not Bold

**Formatted:** Font: 12 pt, Not Bold

**Deleted:** ;

**Deleted:** ,

**Formatted:** Font: 12 pt, Not Bold

**Formatted:** Font: 12 pt, Not Bold

**Formatted:** Font: 12 pt, Not Bold

**Formatted:** Font: 12 pt, Not Bold

**Formatted:** Font: 12 pt, Not Bold

**Formatted:** Font: 12 pt, Not Bold

**Formatted:** Font: 12 pt, Not Bold

**Formatted:** Font: 12 pt, Not Bold

**Formatted:** Font: 12 pt, Not Bold

**Formatted:** Font: 12 pt, Not Bold

**Formatted:** Font: 12 pt, Not Bold

**Formatted:** Font: 12 pt, Not Bold

**Formatted:** Font: 12 pt, Not Bold

**Formatted:** Font: 12 pt, Not Bold

**Deleted:** terrestrial limiting indicators

**Formatted:** Font: 12 pt

**Formatted:** Font: 12 pt, Not Bold

**Deleted:** –

**Formatted:** Font: 12 pt, Not Bold

**Deleted:** (1)

**Deleted:** (2)

**Formatted:** Line spacing: single

**Deleted:** A

**Deleted:** i

**Deleted:** s

**Deleted:** dating

**Deleted:** The east coast of North America and Caribbean sites consist of constructional coral reef terraces and terrestrial eolianites. Most field sites host only an MIS 5a sea level indicator and the common absence of adjacent MIS 5c indicators p(... [1])

**Formatted:** English (US)

**Deleted:** thorium

**Deleted:** date

**Deleted:** thorium

**Deleted:** dates

**Deleted:** terrace

**Deleted:** are

**Deleted:** dates

### 5.3.3 Daebo-Gori region, Korea

875 Choi et al. (2008) utilized differential GPS to map wave-cut **marine platforms** in the Daebo-Gori region. The T2 terrace, with a shoreline angle mapped at 8 – 11 m apsl (Figure 2), is a wide and continuous surface, covered in sediment of up to 2 m thick; the T3b terrace, with a shoreline angle mapped at 17 – 22 m apsl (Figure 3), is a narrow, lower bench of the T3 terrace, separated from the upper bench by a gently sloping riser, which in places makes it difficult to distinguish the two platforms. 16 optically stimulated luminescence **ages** assign the T2 terrace to MIS 5a (Choi et al., 2003; see literature referenced in table 2 of Choi et al., 2008; see Figure 4); eight OSL **ages** and two paleomagnetic **ages** assign the T3b terrace to MIS 5c (Choi et al., 2003; Choi et al., 2008; see literature referenced in table 3 of Choi et al., 2008; see Figure 5).

Deleted: terraces

Formatted: Font: Not Italic

Deleted: l

Deleted: sparsely

Deleted: (OSL)

Deleted: dates

Formatted: Font: Not Italic

Deleted: dates

Deleted: dates

### 5.3.4 Pamilacan Island, Philippines

885 Ringor et al. (2004) mapped the coral reef terraces on Pamilacan Island, for which four uranium-series **ages** on corals have assigned the unnamed broad terrace, with a shoreline angle mapped at 6 m apsl, and the more narrow and poorly developed terrace (also unnamed), with a shoreline angle mapped at 13 m apsl, to MIS 5a and 5c, **respectively**.

Formatted: Font: Not Italic

Deleted: dates

### 5.3.5 Panglao Island, Philippines

890 Omura et al. (2004) mapped the coral reef terraces found along Panglao Island. The lowest well-developed terrace is mapped at 5 m apsl (Figure 3) and is composed of two geomorphic units. The lower unit contains one uranium-series **age** on *Porites* which dates to late MIS 5e. Four uranium-series **ages** on *Platygyra ryukyuensis* assign the upper terrace, of which the inner margin is mapped at 5 m apsl, to MIS 5c (Figure 5).

Formatted: Font: Not Italic

Deleted: date

Formatted: Font: Italic

Deleted: dates

Formatted: Font: Italic

### 895 5.3.6 Tewai and Kwambu Sections, Huon Peninsula

Chappell (1974) first mapped the emergent coral reef terraces along the northern coast of the Huon Peninsula, for which we focus on the well preserved, laterally tilted Va and VIa terraces. 11 uranium-series **ages** on corals and mollusks assign these terraces to MIS 5a and 5c (Veeh and Chappell, 1970; Chappell, 1974; Esat et al., 1999; Cutler et al., 2003; Figures 4 and 5). Chappell and Shackleton (1986) reported the reef crest elevations of the Va and VIa reef terraces to be 260 m apsl and 338 m apsl at the Tewai section and 117 m apsl and 160 m apsl at the Kwambu section (Figures 2 and 3). **Chappell et al. (1996) reconciled Huon Peninsula terrace highstands with oxygen isotope records for the interval spanning 70–30 ka.**

Deleted: dates

Deleted: notably preformed important work

Deleted: ing

Deleted: the

Deleted: record

Deleted: , however the time interval in questions (

Deleted: ) does not fall within the purview of this review

Deleted: dates

### 5.3.7 Hateruma Island, Japan

905 Ota and Hori (1980) proposed an initial chronology for the six lowest Quaternary terraces around Hateruma Island following early mapping efforts discussed in Ota and Omura (1992). Omura (1984) published four uranium-series **ages** on corals that assigned terraces V and IV to MIS 5a and 5c,

respectively (Figures 4 and 5). The updated elevation surveys of Ota and Omura (1992) mapped the maximum height of the terraces V and IV at 23 m apsl and 30 m apsl, respectively (Figures 2 and 3).

### 5.3.8 Atauro Island, East Timor

The lowest two coral reef terraces of Atauro Island, termed 1a and 1b, are mapped at inner edge elevations of 20 m apsl and 36 m apsl, respectively (see literature discussed in Chappell and Veeh, 1978; Chappell and Veeh, 1978; Figures 2 and 3). Two uranium-series ages on corals have assigned terrace 1b to MIS 5c (Figure 5). While no radiometric ages exist for terrace 1a, Chappell and Veeh (1978) used the position of this terrace on age-height plots to infer an age of MIS 5a (Figure 4).

### 5.3.9 Spencer Gulf, Australia

Hails et al. (1984) utilized sediment cores and sonar to study shallow water stratigraphy in the Spencer Gulf, for which we focus on the Lowly Point and False Bay formations. The Lowly Point and False Bay formations occur at water depths exceeding 14 m bpsl and 8 m bpsl, respectively (Figures 2 and 3). No radiometric ages exist for either formation; the stratigraphic position of the Lowly Point and False Bay formations between the MIS 5e age Mambray formation and the Holocene age Germein formation (see literature discussed in Hails et al., 1984), along with the extent to which the depositional events flooded Spencer Gulf, support age assignments of MIS 5a and 5c (Figures 4 and 5).

### 5.3.10 Robe Range, Australia

Sprigg (1952) first mapped the eolianite barrier-shoreline complex of the Robe Range for which we focus on the Robe II and III units. The barrier shoreline is fragmented in some regions and more extensively preserved in areas with higher uplift rates (Murray-Wallace, 2018). Schwebel (1984) reported a barrier shoreline elevation of -6 – 2 m apsl for the Robe II unit (Figure 2); Murray-Wallace (2002) reported the shoreline elevation of Robe III as 2 m bpsl, revised upward from an earlier reported elevation of 15 – 8 m bpsl (Schwebel, 1984) (Figure 3). Comparison between the local stratigraphy and established deep-ocean oxygen isotope records assigns the Robe II and Robe III shorelines to MIS 5a and 5c (Schwebel, 1984). Calibrated amino acid ratios on the Robe III barrier are numerically indistinguishable from the adjacent Robe II barrier which hosts numerical AAR ages that fall within MIS 5a, though the authors note that the AAR method is not able to distinguish specific MIS substages (Blakemore et al., 2015). Based on anomalously young luminescence ages, debate exists in the literature as to whether the Robe II barrier records a true interglacial sea level highstand or formed as a result of local processes (Huntley et al., 1993a; see literature discussed in Huntley et al., 1993a; Banerjee et al., 2003; Murray-Wallace, 2018). We include Robe II in the database as an MIS 5a indicator for completeness, along with the associated anomalously young ages (Figure 4). Four luminescence ages, in conjunction with the stratigraphic position of the Robe III unit, supports an age assignment of MIS 5c (Huntley et al., 1993b; Huntley et al., 1994; Huntley and Prescott, 2001; Banerjee et al., 2003; Figure 5).

Deleted: dates

Deleted: dates

Formatted: Font: Not Italic

Deleted: dates

Deleted: n

Deleted: of

Deleted:

Deleted:

Deleted: if

Deleted: more

Deleted: dates

Deleted: A single

Deleted: date

### 5.3.11 Makran Subduction Zone, Iran (Lipar, Ramin, Gurdim, Jask sites)

975 Harrison (1941) first documented the marine terraces along the Makran subduction zone of Iran;  
subsequent authors extended the initial mapping, documenting the differential uplift and lateral tilting of  
980 the terraces (Page et al., 1979; Reyss et al., 1998; Normand et al., 2019). Normand et al. (2019)  
revisited the terraces and provided updated elevations for the terraces found at the Lipar, Ramin,  
Gurdim, Jask sites. The majority of the T1 terraces, dated with three optically stimulated luminescence  
| ages and a single uranium-series age to MIS 5a (Figure 4), have a shoreline angle mapped at 2 m bpsl to  
980 65 m apsl (Normand et al., 2019; Figure 2). Normand et al. (2019) expanded on the history of the T1  
terrace at the Ramin site, which hosts two luminescence samples dated to MIS 5e and 5a, respectively,  
concluding that the chronology implies a reoccupation of the T1 terrace during multiple sea level  
| highstands (Figure 4). The Lipar site also contains a T2 terrace mapped at 45 m apsl (Figure 2) which  
hosts a luminescence sample dated to MIS 5a (Figure 4).

Deleted: dates

Deleted: date

Deleted: high stand

### 985 5.3.12 The Gulf of Gabes, Tunisia

Gzam et al. (2016) utilized high precision echo sounders to map two submerged beach ridges, with peak  
elevations of 8 m and 19 m bpsl (Figure 2 and 3). From their analysis of biocalcarenite development,  
the authors concluded that the ridge formation could indicate a rapid sea level transgression which,  
along with the stratigraphic position of the 8 m and 19 m ridges, supported their respective age  
990 assignments of MIS 5a and 5c (Figure 4 and 5). At present, no radiometric ages exist for these beach  
ridges.

Deleted: dates

Formatted: English (UK)

Formatted: Normal

Deleted: for

Formatted: English (UK)

Formatted: English (UK)

Deleted: ;

Formatted: English (UK)

Formatted: English (UK)

Formatted: English (UK)

Deleted: ;

Formatted: English (UK)

Deleted: ,

Formatted: English (UK)

Deleted: ,

Formatted: English (UK)

Formatted: English (UK)

Deleted: ;

Formatted: English (UK)

Formatted: English (UK)

Deleted: ,

### 5.3.13 Summary

995 Sea level indicators in the far field encompass marine terraces, coral reef terraces, and both marine and  
terrestrial limiting indicators (shallow water facies and beach ridges, respectively), which have quality  
ratings between average (3) and rejected (0) (Figures 6c,f; Tables 1 and 2). As with the previous two  
regions, we used IMCalc to quantify the indicative meaning of each relative sea level indicator in the  
absence of reported modern analog data (WALIS RSL IDs 3520–3537, 3557–3562, 3982; Lorscheid  
and Rovere, 2019). Most primary references do not report a clear reference datum, which limits the  
maximum quality rating to average (3). An average (3) rating for a coral reef terrace typically reflects  
000 both a precise measurement and a narrow indicative range (less than ~2 m) as calculated by IMCalc (as  
for MIS 5a and 5c indicators at Pamilacan Island and Hateruma Island and the MIS 5c indicator at  
Panglao Island). In contrast, as marine terraces typically have larger indicative ranges, an average (3)  
quality rating necessitates a precise elevation measurement (e.g., the MIS 5a and 5c indicators at  
005 Daebo-Gori region and the MIS 5a indicators at Lipar and Gurdim). Poor ratings (2) for marine and  
coral reef terraces arise from imprecise measurements, intrinsic to survey methods such as altimeters and  
topographic maps, or from not reporting measurement uncertainty (such as the MIS 5a and 5c indicators  
at Bahía Inglesa, Oahu, Atauro Island, Tewai Section, Kwambu Section and MIS 5a indicators at  
Ramin and Jask). All sites in Tunisia and Australia receive rejected (0) quality ratings because they only  
provide minimum/maximum limiting constraints on paleo-sea level. In summary, we advocate for





Marine Isotone Stage 5a							
Site	Latitude	Longitude	Elevation	Indicator Type <sup>1</sup>	Dating Method	Indicator Quality	Age Quality
Newport	44.63	-124.05	(0 - 45) ± 3.3	SLI	AAR, Other	1	2
Cape Arago	43.306531	-124.401657	31 ± 2	SLI	Other	2	2
Coquille Point	43.114117	-124.437096	18 ± 2	SLI	U-Series, AAR	2	4
Brookings	42.05	-124.28	(30 - 62) ± 6	SLI	Other	1	2
Bruhel Point	39.607469	-123.786856	10 ± 2	SLI	Stratigraphy, AAR	2	2
Point Reyes	37.9	-122.6938	(38 - 77) ± 3.4	SLI	Luminescence	1	4
Santa Cruz (Western terrace)	36.96	-122.09	87 ± 3.3	SLI	Other	2	3
Santa Cruz (Davenport terrace)	37.0294755	-122.1923133	(5 - 10)	SLI	U-Series, AAR, Other	2	4
San Simeon <sup>2</sup>	35.639462	-121.1848936	(5 - 24) ± 2	SLI	U-Series, Luminescence, Other	1	3
Point Buchon	35.2552529	-120.8990702	(5 - 14) ± 2	SLI	U-Series, Other	1	2
Gaviota	34.4675398	-120.2674989	(10 - 17) ± 2	SLI	U-Series, AAR, Other	2	2
Santa Rosa Island	34.003812	-120.195602	(5.4 - 7.4) ± 1	SLI	AAR	2	2
San Miguel Island	34.0191768	-120.3177209	3.5	SLI	Stratigraphy	2	2
Palos Verdes Hills	33.7246996	-118.3552086	(45 - 47)	SLI	U-Series, AAR	2	4
San Joaquin Hills	33.5696784	-117.8385408	(19 - 22)	SLI	U-Series	2	3
San Nicolas Island	33.2472453	-119.5070695	(8 - 13) ± 0.3	SLI	U-Series	2	4
Oceanside	33.17	-117.35	(9 - 11) ± 2	SLI	AAR	2	2
Point Loma	32.67	-117.24	(9 - 11) ± 2	SLI	U-Series, AAR	2	3
Punta Banda	31.7455541	-116.7394247	(15 - 17.5) ± 0.2	SLI	U-Series	3	4
Punta Cabras	31.33	-116.44	(4.5 - 17)	SLI	Other	1	3
Virgina Beach	36.7823	-76.1966	7.5 ± 3	SLI	U-Series, AAR, ESR	3	4
Moyock	36.508	-76.153	5 ± 3	SLI	U-Series	3	4
Pamlico Sound	35.4828287	-75.951469	(9 - 14)	SLI	Luminescence	2	4
Charleston	32.8586	-79.7803	5 ± 3	SLI	U-Series	3	4
Skidaway	31.916	-81.071	3 ± 3	SLI	U-Series	2	4
Freeport Rocks	27.7852552	-96.9132876	-18.9	TL	Luminescence	0	4
Fort St. Catherine	32.390733	-64.674732	(1 - 2) ± 1	TL	U-Series, AAR	0	4
Sand Key Reef	24.4977811	-81.8477838	(-12 - -10)	SLI	U-Series	3	4
Eleuthera Is.	25.0090818	-76.3780482	(-5 - -25)	SLI	AAR	3	2
Northwestern Peninsula	19.8039797	-73.3097345	23.4	SLI	U-Series	2	4

Christ Church	13.0699141	-59.5693843	3 +1/-2	SLI	U-Series, Other	4	4
Clermont Nose	13.1350465	-59.6345479	20 +3/-2	SLI	U-Series, Other	3	3
Southern Coast	13.0698341	-59.5409821	(2 - 3) ± 1	SLI	U-Series, ESR	3	4
Oahu	21.4477881	-158.1997812	(-30 - -20)	SLI	U-Series	2	4
Bahía Inglesa	-27.1142508	-70.8742622	10 ± 5	SLI	Stratigraphy	2	2
Daebo-Gori Region	36.0554812	129.5444388	(8 - 11)	SLI	Luminescence	3	2
Pamilaçan Island	9.4951118	123.9281264	6 ± 1	SLI	U-Series	3	4
Tewai Section	-6.2206748	147.6766172	260	SLI	U-Series, Stratigraphy	2	4
Kwambu Section	-6.0704502	147.5171788	117	SLI	U-Series, Stratigraphy	2	3
Hateruma Island	24.058648	123.7817205	23 ± 2	SLI	U-Series	3	3
Atauro Island	-8.3012532	125.5565624	20	SLI	Other	2	2
Lipar	25.2567922	60.80393	20 ± 2.1	SLI	U-Series, Luminescence	3	4
Lipar	25.2591769	60.7979098	45 ± 2.1	SLI	Luminescence	3	4
Ramin	25.2694195	60.763467	-2 ± 4.3	SLI	Luminescence	2	3
Gurdim	25.3390736	60.1665682	62 ± 2.1	SLI	Luminescence	3	4
Jask	25.6552358	57.7874395	-3 ± 4.3	SLI	Luminescence	2	4
Bsissi	33.7171283	10.313814	-8 ± 1	TL	Stratigraphy	0	2
Ghannouche	33.7072534	10.3343664	-9 ± 1	TL	Stratigraphy	0	2
Teboulbou	33.7007635	10.3519874	-8 ± 1	TL	Stratigraphy	0	2
Kettana	33.6785967	10.4125647	-9 ± 1	TL	Stratigraphy	0	2
Zarat	33.6785967	10.4125647	-8 ± 1	TL	Stratigraphy	0	2
Zerkine	33.6785967	10.4125647	-18 ± 1	TL	Stratigraphy	0	2
Spencer Gulf	-33.9120079	136.8615574	-8	ML	Other	0	2
Robe Range	-37.219789	139.787838	(-6 - 2)	TL	AAR, Other	0	2

070

Deleted: ¶

Deleted: Marine Isotope Stage 5a

... [2]

075

Table 2: \*SLI = Sea Level Indicator, TL = Terrestrial Limiting, ML = Marine Limiting

Deleted: Marine Isotope Stage 5c

... [3]

Deleted: Marine Isotope Stage 5c

... [4]

Marine Isotope Stage 5c							
Site	Latitude	Longitude	Elevation	Indicator Type <sup>1</sup>	Dating Method	Indicator Quality	Age Quality
Newport	44.63	-124.05	(0 - 85) ± 6	SLI	Other	1	2
Cape Arago	43.306531	-124.401657	68 ± 2	SLI	Stratigraphy	2	2
Coquille Point	43.114117	-124.437096	70 ± 2	SLI	Stratigraphy	2	2
Brookings	42.05	-124.28	(57 - 90) ± 6	SLI	Other	1	2
Bruhel Point	39.607469	-123.786856	23 ± 2	SLI	Stratigraphy	2	2
Santa Cruz (Wilder terrace)	36.96	-122.09	132 ± 3.3	SLI	Other	2	3
Santa Cruz (Highway 1 terrace)	37.0294755	-122.1923133	26	SLI	Other	1	2
Gaviota	34.4675398	-120.2674989	25 ± 5	SLI	AAR, Other	2	2
San Nicolas Island	33.2472453	-119.5070695	(28 - 33) ± 0.3	SLI	U-Series	2	3
Malibu	34.03	-118.71	(7.6 - 39.6)	SLI	U-Series	1	3
Punta Banda	31.7455541	-116.7394247	22 ± 0.2	SLI	Stratigraphy	3	2
Fort St. Catherine	32.390733	-64.674732	Not Reported	TL	U-Series, AAR	0	3
Berry Island	25.6250042	-77.8252203	(0.2 - 2.3) ± 1	SLI	U-Series	4	3
Northwestern Peninsula	19.8039797	-73.3097345	37.2	SLI	U-Series	2	4
Christ Church	13.0699141	-59.5693843	6 +5/-1	SLI	U-Series, Other	2	4
Clermont Nose	13.1350465	-59.6345479	30 +3/-2	SLI	U-Series, Other	3	4
Southern Coast	13.0698341	-59.5409821	(4 - 16) ± 1	SLI	U-Series, ESR	2	4
Oahu	21.4477881	-158.1997812	(-30 - -20)	SLI	U-Series	2	4
Bahía Inglesa	-27.1142508	-70.8742622	31 ± 5	SLI	Stratigraphy	2	2
Daobo-Gori Region	36.0554812	129.5444388	(17 - 22)	SLI	Luminescence, Other	3	2
Pamilacan Island	9.4951118	123.9281264	13 ± 1.6	SLI	U-Series	3	4
Panglao Island	9.573798	123.8221394	5	SLI	U-Series	3	4
Tewai Section	-6.2206748	147.6766172	338	SLI	Stratigraphy	2	2
Kwambu Section	-6.0704502	147.5171788	160	SLI	U-Series, Stratigraphy	2	3
Hateruma Island	24.058648	123.7817205	30 ± 2	SLI	U-Series	3	4
Atauro Island	-8.3012532	125.5565624	36	SLI	U-Series	2	4
Zarat	33.6785967	10.4125647	-18 ± 1	TL	Stratigraphy	0	2
Zerkine	33.6785967	10.4125647	-20 ± 1	TL	Stratigraphy	0	2
Spencer Gulf	-33.9120079	136.8615574	-14	ML	Other	0	2

Formatted Table

## 6 Review of Research Themes on MIS 5a and 5c RSL Indicators and Future Research Directions

085 The global database of sea level indicators dated (or assigned) to MIS 5a and 5c presented in this paper reasonably covers the Pacific coast of North America (18 field sites), the Atlantic coast of North America and the Caribbean (9 field sites), and more sparsely covers the remaining globe (12 field sites). The broad geographic spread of the data allows for an increasingly resolved reconstruction of MIS 5a and 5c GMSL sea level, with especially good coverage in the near field of the North American Ice Sheets. Future efforts could expand this database by including additional indicators reported outside of North America, particularly those reported in non-English language journals.

090 Two complementary research themes rely upon MIS 5 relative sea level indicators with unequivocal substage chronology and robust elevation data. One focus leverages the spatial variation in reconstructions of local MIS 5a and 5c RSL elevations to constrain global geophysical models for glacial isostatic adjustment and, hence, to refine estimates of substage global mean sea level (GMSL; e.g., Lambeck and Chappell, 2001; Potter and Lambeck, 2004; Muhs et al., 2012; Creveling et al., 2017). The other focus deduces regional rates of tectonic motion from the vertical displacement of (MIS 5e) RSL indicators from the sea level at which they formed (e.g., Matthews, 1973; Chappell, 1974; Wehmiller et al., 1977; Muhs et al., 1990, 1992b; Simms et al., 2016). Numerous field and numerical analyses highlight the entanglement of these themes. Robust efforts to deduce MIS 5a and 5c GMSL from misfit analyses between field observational data and GIA models necessitate a quantitative correction for a site's tectonic uplift history (Creveling et al., 2015; Simms et al., 2016). Inasmuch as a vertical tectonic uplift correction requires a robust paleo-sea level reference datum, this reference datum should reflect the estimates of interstadial GMSL and melt-induced spatial variations in local sea level from glacial isostatic adjustment models (Creveling et al., 2015; Simms et al., 2016). Advances in each research theme enrich the other, and both rely upon RSL indicators with high quality elevation measurements and substage-resolution chronology.

110 Tectonic uplift-corrected RSL indicators in the near-to-intermediate field of the North American ice complex display distinct geographic trends arising from glacial isostatic adjustment (Potter and Lambeck, 2004; Simms et al., 2016). North American Atlantic coast and Caribbean MIS 5a highstand elevations display a north-to-south latitudinal gradient that decreases by ~30 m elevation (Cronin et al., 1981; Szabo, 1985; Bard et al., 1990; Cutler et al., 2003; Potter et al., 2004; Wehmiller et al., 2004; Parham et al., 2013). Potter and Lambeck (2004) demonstrated that this trend reflects the glacio-isostatic disequilibrium imposed by the forebulge of the Laurentide ice sheet. After correcting Atlantic Coast and Caribbean RSL inferences for glacioisostasy, Potter and Lambeck (2004) concluded that MIS 5a GMSL peaked ~-28 m below present (with a similar value for MIS 5c). Potter and Lambeck (2004) predicted broadly consistent magnitudes, though narrower bounds, on MIS 5a and 5c substage GMSL as Lambeck and Chappell (2001) who reconstructed GMSL of 23–37 m and 18–30 m below present, respectively, from Huon Peninsula coral reef terraces. In contrast, tectonic uplift- and GIA-corrected MIS 5a and MIS 5c RSL indicators along the Pacific coast of the U.S. and Mexico reveal an opposing latitudinal gradient in local high-stand elevations from that observed on the North American Atlantic coast and Caribbean (Simms et al., 2016). On the basis of the North American Pacific coast geographic

Formatted: Font: 12 pt

Formatted: Line spacing: single

Deleted: substage

Deleted: Cronin et al., 1981

Formatted: Default Paragraph Font, Font: 12 pt

Formatted: Font: 12 pt

Deleted: Szabo, 1985

Deleted: Bard et al., 1990

Deleted: Potter et al., 2004

Formatted: Default Paragraph Font, Font: 12 pt

Formatted: Font: 12 pt

Deleted: Wehmiller et al., 2004

Formatted: Default Paragraph Font, Font: 12 pt

Formatted: Font: 12 pt

Formatted: Default Paragraph Font, Font: 12 pt

Formatted: Font: 12 pt

Deleted: Cutler et al., 2003

Formatted: Default Paragraph Font, Font: 12 pt

Formatted: Font: 12 pt

Formatted: Default Paragraph Font, Font: 12 pt

Formatted: Font: 12 pt

Deleted: Parham et al., 2013

Formatted: Default Paragraph Font, Font: 12 pt

Formatted: Font: 12 pt

Deleted: Potter and Lambeck (2004)

Formatted: Default Paragraph Font, Font: 12 pt

Formatted: Font: 12 pt

Deleted: Lambeck and Chappell (2001)

Formatted: Default Paragraph Font, Font: 12 pt

Formatted: Font: 12 pt

135 gradient, Simms et al. (2016) concluded that MIS 5 and 5c peak GMSL reached up to  $\sim 15$  m and  $\sim$   
10 m below present sea level, a conclusion in agreement with that of Muhs et al. (2012) who  
140 reconstructed peak GMSL elevations of  $\sim 16$  m and  $\sim 9$  m during MIS 5a and MIS 5c, respectively, based  
on tectonic uplift- and GIA-corrected RSL indicators at San Nicolas Island, California; the Florida  
Keys; and Barbados.

140 The opposing latitudinal gradients in MIS 5a and 5c peak highstand elevations imposed by the  
peripheral bulge of the North American ice complex do not find reconciliation with conventional '1-D'  
145 glacial isostatic adjustment models that assume a depth-varying but laterally homogenous viscoelastic  
structure (Creveling et al., 2017). Notably, embedding an upper mantle viscosity in a GIA models to  
reconcile the highstand latitudinal gradient from one geographic region (i.e., the Pacific or Atlantic  
150 coast of North America) exacerbates the misfit of GIA predictions to the RSL indicators of the other  
region. Hence, GIA analyses that focus on a regional subset of global data produce GMSL estimates  
with systematic errors (hence the conflicting GMSL predictions of Potter and Lambeck (2004) versus  
155 Simms et al. (2016)). Creveling et al. (2017) promoted the adoption of a sensitivity analysis between  
globally distributed RSL indicators and GIA predictions that adopt viscosity models that honor the  
complexity in (North American) upper mantle viscosity. The resulting analytical workflow, applied to  
an unfiltered compendium of MIS 5a and 5c RSL indicators, yielded peak GMSL bounds of  $-18 \pm 1$  m  
and  $-20 \pm 1$  m for MIS 5a and MIS 5c, respectively; notably, repeating this sensitivity analysis on a RSL  
database filtered to include only those with high-quality (predominately uranium-series) chronology  
widened these bounds to  $-22 \pm 1$  m and  $-24 \pm 2$  m, respectively (Creveling et al., 2017).

Continued refinement of MIS 5a and 5c peak GMSL and regional rates of Quaternary vertical tectonic  
uplift remains within reach. First, numerical models for glacial isostatic adjustment that adopt '3D'  
160 solid earth models with depth-varying and laterally homogenous viscoelastic structure promise to  
reconcile observed spatial gradients in RSL highstands and GIA model predictions (e.g., Latychev et al.,  
2005; Clark et al., 2019). Such numerical advancements offer the possibility of refining GMSL  
estimates in the absence of further field data collection. Second, the quality ratings conferred above  
165 motivate the strategic re-surveying of a subset of MIS 5a and 5c field observations (see Sections 5.1.19,  
5.2.10, and 5.3.13) in order that each site conform to the uniform approach to establishing the elevation  
and uncertainty of elevation measurements ages adopted for the World Atlas of Last Interglacial Sea  
Level (e.g. Rovere et al., 2016). The re-sampling and/or re-analysis of geochronological material may  
also refine the numerical ages adopted for the World Atlas of Last Interglacial Sea Level (e.g. Rovere  
170 et al., 2016). Importantly, this retroactive translation of MIS 5a and 5c RSL observations to rigorous sea-  
level index points (*sensu* Hijma et al., 2015) offers the paired promise of refining predictions of  
contemporaneous global mean sea level and vertical tectonic motion and the standardization of efforts  
to complete these research foci. Third, the proliferation of airborne LiDAR data can offer geoscientists a  
fresh perspective on the quantity and spatial relationships of purported terrace platforms (Bowles and  
175 Cowgill, 2012) that, once ground-truthed, may confer confidence in, or contradict, chronologies  
developed from terrace counting methods. In practice, simultaneous efforts to enact all three practices  
will enrich conclusions about MIS 5a and 5c GMSL bounds and the accompanying tectonic  
displacement of these RSL indicators.

Deleted: -

Deleted: -

Deleted: Muhs et al. (2012)

Formatted: Default Paragraph Font, Font: 12 pt

Formatted: Font: 12 pt

Deleted: -

Deleted: -

Deleted: upper mantle

Deleted: concluded that

Deleted: peaked at

Deleted: during

Deleted: U

Deleted: s

Deleted: X

Deleted: Y

Deleted: Z

Formatted

Formatted: Normal

**Deleted:** The global database of sea level indicators dated (or assigned) to MIS 5a and 5c presented in this paper reasonably densely covers the Pacific coast of North America (18 field sites), the Atlantic coast of North America and the Caribbean (9 field sites), and more sparsely covers the remaining globe (12 field sites). The broad geographic spread of the data allows for an increasingly resolved reconstruction of MIS 5a and 5c GMSL sea level, with especially good coverage in the near field of the North American Ice Sheets. Future research directions could address scant indicators reported (in English language journals) outside of North America, and refine radiometric chronologies for existing indicators.

## 7 Data Availability

The database detailed in this study is available at <https://doi.org/10.5281/zenodo.4426206> (Thompson and Creveling, 2021). The content at this link were exported from the WALIS database interface on 7  
195 January 2020. A summary of these WALIS data can be found in Tables 1 and 2 of this manuscript. Description of each data field in the database is contained at this link: <https://doi.org/10.5281/zenodo.3961543> (Rovere et al., 2020). More information on the World Atlas of Last Interglacial Shorelines can be found here: <https://warmcoasts.eu/world-atlas.html>. Users of this database are encouraged to cite the primary literature sources as well as this article.

200 **Author Contribution** S.T. assumed primary responsibility for all entries into the WALIS database, and the illustration of these data. S.T. extended the literature review of MIS 5a and 5c indicators beyond that reported in Creveling et al. (2017). S.T. and J.R.C. contributed equally to the structure and writing of the manuscript.

**Competing Interests** The authors declare that they have no conflict of interest.

## Special Issue Statement

205 **Acknowledgments** The data presented in this publication were compiled in WALIS, a sea-level database interface, developed with funding from the ERC Starting Grant “WARMCOASTS” (ERC-StG-802414), in collaboration with PALSEA (PAGES/INQUA) Working Group. The database structure was designed by A. Rovere, D. Ryan, T. Lorscheid, A. Dutton, P. Chutcharavan, D. Brill, N. Jankowski, D. Mueller, M. Bartz, E. Gowan and K. Cohen. The authors wish to thank Daniel Muhs for clarifying innumerable aspects of MIS 5a and 5c field observation and geochronological caveats over many  
210 years of conversation and [Colin Murray-Wallace, one anonymous referre, and Alessio Rovere](#) for constructive comments on manuscript drafts and database entries.

## References

- 225 Adams, J.: Active deformation of the Pacific Northwest Continental Margin, *Tectonics*, 3, 449–472, <https://doi.org/10.1029/TC003i004p00449>, 1984.
- Addicott, W.O., Emerson, W.K.: Late Pleistocene Invertebrates from Punta Cabras, Baja California, Mexico. *American Museum Novitates*, 1925, 1–34, 1959.
- Alexander, C. S.: The marine and stream terraces of the Capitola-Watsonville area, University of California Publications in Geology, 1953.
- 230 Allen, C. R., Silver, L. T., and Stehli, F. G.: Agua Blanca fault—A major transverse structure of northern Baja California, Mexico, *Geol Soc Am Bull*, 71, 457–482, [https://doi.org/10.1130/0016-7606\(1960\)71\[467:ABFMTS\]2.0.CO;2](https://doi.org/10.1130/0016-7606(1960)71[467:ABFMTS]2.0.CO;2), 1960.
- 235 [Banerjee, D., Hildebrand, A.N., Murray-Wallace, C. V., Bourman, R.P., Brooke, B.P., Blair, M.: New quartz SAR-OSL ages from the stranded beach dune sequence in south-east South Australia. \*Quaternary Sci Rev\*, 22, 1019–1025, 2003.](#)
- [Bard, E., Hamelin, B., Fairbanks, R.G.: U-Th ages obtained by mass spectrometry in corals from Barbados: Sea level during the past 130,000 years. \*Nature\*, 346, 456–458, 1990.](#)
- Barnes, J.W., Lang, E.J., Potratz, H.A.: Ratio of ionium to uranium in coral limestone, *Science*, 124, 175–176, 1956.
- 240 Bender, M.L., Fairbanks, R.G., Taylor, F.W., Matthews, R.K., Goddard, J.G., and Broecker, W.S.: Uranium-series dating of the Pleistocene reef tracts of Barbados, West Indies, *Bull Geol Soc Am*, 90, 577–594, [https://doi.org/10.1130/0016-7606\(1979\)90<577:UDOTPR>2.0.CO;2](https://doi.org/10.1130/0016-7606(1979)90<577:UDOTPR>2.0.CO;2), 1979.
- Berger, G.W., Hanson, K.L.: Thermoluminescence Ages of Estuarine Deposits Associated With Quaternary Marine Terraces, South-Central California, in: *Quaternary coasts of the United States*, edited by: Fletcher, C.H., Wehmiller, J.F., 303–308, 1992.
- 245 Birkeland, P.W.: Late Quaternary Eustatic Sea-Level Changes along the Malibu Coast, Los Angeles County, California, *The Journal of Geology*, 80, 432–448, <https://doi.org/10.1086/627765>, 1972.
- 250 [Blakemore, A.G., Murray-Wallace, C. V., Westaway, K.E., Lachlan, T.J.: Aminostratigraphy and sea-level history of the Pleistocene Bridgewater Formation, Mount Gambier region, southern Australia. \*Aust J Earth Sci\*, 62, 151–169, 2015.](#)
- [Bowles, C.J. and Cowgill, E.: Discovering marine terraces using airborne LiDAR along the Mendocino-Sonoma coast, northern California. \*Geosphere\*, 8, 2, 386–402. <https://doi.org/10.1130/GES00702.1>, 2012.](#)
- 255 Bradley, W.C. and Addicott, W.O.: Age of First Marine Terrace Near Santa Cruz, California, *Geol Soc Am Bull*, 79, 1203–1210, [https://doi.org/10.1130/0016-7606\(1968\)79\[1203:AOFMTN\]2.0.CO;2](https://doi.org/10.1130/0016-7606(1968)79[1203:AOFMTN]2.0.CO;2), 1968.
- Bradley, W.C. and Griggs, G.B.: Form, genesis, and deformation of central California wave-cut platforms, *Bull Geol Soc Am*, 87, 433–449, [https://doi.org/10.1130/0016-7606\(1976\)87<433:FGADOC>2.0.CO;2](https://doi.org/10.1130/0016-7606(1976)87<433:FGADOC>2.0.CO;2), 1976.
- 260 Bretz, J.H.: Bermuda: A Partially Drowned, Late Mature, Pleistocene Karst, *Bull Geol Soc Am*, 71, 1729–1754, 1960.
- Broecker, W.S., Thurber, D.L.: Uranium-series dating of corals and oolites from Bahaman and Florida Key limestones, *Science*, 149, 58–60, 1965.

Deleted: ence

Deleted: iews

Formatted: English (US)

Formatted: English (US)

Formatted: Font: Not Italic

Formatted: English (US)

- Broecker, W.S., Thurber, D.L., Goddard, J., Ku, T.L., Matthews, R.K., and Mesoella, K.J.:  
Milankovitch hypothesis supported by precise dating of coral reefs and deep-sea sediments, *Science*,  
159, 297–300, <https://doi.org/10.1126/science.159.3812.297>, 1968.
- Carter, G. F.: *Pleistocene man at San Diego*, Johns Hopkins Press, Baltimore, 400, 1957.
- 270 Chappell, J.: Geology of coral terraces, Huon Peninsula, New Guinea: A study of Quaternary tectonic  
movements and sea-level changes, *Bull Geol Soc Am*, 85, 553–570, [https://doi.org/10.1130/0016-7606\(1975\)86<1482:GOCTHP>2.0.CO;2](https://doi.org/10.1130/0016-7606(1975)86<1482:GOCTHP>2.0.CO;2), 1974.
- Chappell, J. and Shackleton, N.J.: Oxygen isotopes and sea level, *Nature*, 324, 137–140,  
<https://doi.org/10.1038/324137a0>, 1986.
- 275 Chappell, J. and Veeh, H.H.: Late Quaternary tectonic movements and sea-level changes at Timor and  
Atauro Island, *Bull Geol Soc Am*, 89, 356–368, [https://doi.org/10.1130/0016-7606\(1978\)89<356:LQTMAS>2.0.CO;2](https://doi.org/10.1130/0016-7606(1978)89<356:LQTMAS>2.0.CO;2), 1978.
- 280 [Chappell, J., Omura, A., Esat, T., McCulloch, M., Pandolfi, J., Ota, Y., Pillans, B.: Reconciliation of late Quaternary sea levels derived from coral terraces at Huon Peninsula with deep sea oxygen isotope records. \*Earth Planet Sc Lett\*, 141, 227–236, 1996.](#)
- Choi, J.H., Murray, A.S., Jain, M., Cheong, C.S., and Chang, H.W.: Luminescence dating of well-sorted  
marine terrace sediments on the southeastern coast of Korea, *Quaternary Sci Rev*, 22, 407–421,  
[https://doi.org/10.1016/S0277-3791\(02\)00136-1](https://doi.org/10.1016/S0277-3791(02)00136-1), 2003.
- Choi, S.J., Merritts, D.J., and Ota, Y.: Elevations and ages of marine terraces and late Quaternary rock  
uplift in southeastern Korea, *J Geophys Res-Sol Ea*, 113, 1–15, <https://doi.org/10.1029/2007JB005260>,  
2008.
- 285 [Chutcharavan, P. and Dutton, A.: A Global Compilation of U-series Dated Fossil Coral Sea-level Indicators for the Last Interglacial Period \(MIS 5e\). \*Earth Syst Sci Data\*, 1–41, 2021, accepted.](#)
- 290 [Clark, J., Mitrovica, J.X. Latychev, K.: Glacial isostatic adjustment in central Cascadia: Insights from three-dimensional Earth modeling. \*Geology\*, 47, 4, 295–298, <https://doi.org/10.1130/G45566.1>, 2019.](#)
- Creveling, J.R., Mitrovica, J.X., Hay, C.C., Austermann, J., Kopp, R.E.: Revisiting tectonic corrections  
applied to Pleistocene sea-level highstands, *Quaternary Sci Rev*, 111, 72–80, 2015.
- Creveling, J.R., Mitrovica, J.X., Clark, P.U., Waelbroeck, C., and Pico, T.: Predicted bounds on peak  
global mean sea level during marine isotope stages 5a and 5c, *Quaternary Sci Rev*, 163, 193–208,  
295 <https://doi.org/10.1016/j.quascirev.2017.03.003>, 2017.
- Cronin, T.M., Szabo, B.J., Ager, T.A., Hazel, J.E., and Owens, J.P.: Quaternary climates and sea levels  
of the U.S. Atlantic coastal plain, *Science*, 211, 233–240, <https://doi.org/10.1126/science.211.4479.233>,  
1981.
- Cutler, K.B., Edwards, R.L., Taylor, F.W., Cheng, H., Adkins, J., Gallup, C.D., Cutler, P.M., Burr,  
300 G.S., and Bloom, A.L.: Rapid sea-level fall and deep-ocean temperature change since the last  
interglacial period, *Earth Planet Sc Lett*, 206, 253–271, [https://doi.org/10.1016/S0012-821X\(02\)01107-X](https://doi.org/10.1016/S0012-821X(02)01107-X), 2003.
- Davis, W.M.: Glacial epochs of the Santa Monica Mountains, California, *P Natl Acad Sci USA*, 18,  
659–665, <https://doi.org/10.1073/pnas.18.11.659>, 1932.
- 305 Dibblee Jr., T.W., Ehrenspeck, H.E.: General geology of Santa Rosa Island, California. In:  
Contributions to the Geology of the Northern Channel Islands, Southern California, edited by: Weigand,  
P.W., Bakersfield, California, Pacific Section American, 1998.

Formatted: English (US)

Deleted: .

Deleted: 0

Deleted: in review

Formatted: Font: Not Italic

Field Code Changed

Formatted: English (US)



- Dodge, R.E., Fairbanks, R.G., Benninger, L.K., and Murrassa, F.: Pleistocene sea levels from raised coral reefs of Haiti, *Science*, 219, 1423–1425, <https://doi.org/10.1126/science.219.4591.1423>, 1983.
- Duller, G.A.T.: Luminescence dating of Quaternary sediments: Recent advances, *J Quaternary Sci*, 19, 183–192, <https://doi.org/10.1002/jqs.809>, 2004.
- 315 Dumas, B., Hoang, C.T., and Raffy, J.: Record of MIS 5 sea-level highstands based on U/Th dated coral terraces of Haiti, *Quatern Int*, 145–146, 106–118, <https://doi.org/10.1016/j.quaint.2005.07.010>, 2006.
- Dutton, A., Lambeck, K.: Ice Volume and Sea Level During the Last Interglacial, *Science*, 216, 216–220, <https://doi.org/10.1126/science.1205749>, 2012.
- Dutton, A., Carlson, A.E., Long, A.J., Milne, G.A., Clark, P.U., DeConto, R., Horton, B.P., Rahmstorf, S., Raymo, M.E.: Sea-level rise due to polar ice-sheet mass loss during past warm periods, *Science*, 349, <https://doi.org/10.1126/science.aaa4019>, 2015.
- Edwards, R.L., Cheng, H., Murrell, M.T., and Goldstein, S.J.: Protactinium-231 dating of carbonates by thermal ionization mass spectrometry: Implications for quaternary climate change, *Science*, 276, 782–786, <https://doi.org/10.1126/science.276.5313.782>, 1997.
- β25 Ellis, A. J.: Physiography, in: *Geology and ground waters of the western part of San Diego County, California*, U.S. Geol. Survey Water-Supply Paper, 446, 20-50, 1919.
- Esat, T.M., McCulloch, M.T., Chappell, J., Pillans, B., and Omura, A.: Rapid fluctuations in sea level recorded at Huon Peninsula during the penultimate deglaciation, *Science*, 283, 197–201, <https://doi.org/10.1126/science.283.5399.197>, 1999.
- 330 Grant, L.B., Mueller, K.J., Gath, E.M., Cheng, H., Edwards, R.L., Munro, R., and Kennedy, G.L.: Late Quaternary uplift and earthquake potential of the San Joaquin Hills, southern Los Angeles basin, California, *Geology*, 27, 1031–1034, [https://doi.org/10.1130/0091-7613\(1999\)027<1031:LQUAEP>2.3.CO;2](https://doi.org/10.1130/0091-7613(1999)027<1031:LQUAEP>2.3.CO;2), 1999.
- Griggs, A.B.: Chromite-Bearing Sands of the Southern Part of the Coast of Oregon, *Geological Survey Bulletin*, 1944, 113–150, 1945.
- 335 Grove, K., Sklar, L.S., Scherer, A.M., Lee, G., and Davis, J.: Accelerating and spatially-varying crustal uplift and its geomorphic expression, San Andreas Fault zone north of San Francisco, California, *Tectonophysics*, 495, 256–268, <https://doi.org/10.1016/j.tecto.2010.09.034>, 2010.
- Gzam, M., Mejdoub, N. El, and Jedoui, Y.: Late quaternary sea level changes of gables coastal plain and shelf: Identification of the MIS 5c and MIS 5a onshore highstands, Southern Mediterranean, *J Earth Syst Sci*, 125, 13–28, <https://doi.org/10.1007/s12040-015-0649-7>, 2016.
- 340 Hails, J.R., Belperio, A.P., and Gostin, V.A.: Quaternary sea levels, northern Spencer Gulf, Australia, *Mar Geol*, 61, 373–389, [https://doi.org/10.1016/0025-3227\(84\)90175-0](https://doi.org/10.1016/0025-3227(84)90175-0), 1984.
- Hanks, T.C., Bucknam, R.C., Lajoie, K.R., and Wallace, R.E.: Modification of Wave-Cut and Faulting-345 Controlled Landforms, *J Geophys Res*, 89, 5771–5790, <https://doi.org/10.1029/JB089iB07p05771>, 1984.
- Hanson, K.L., Lettis, W.R., Wesling, J.R., Kelson, K.I., and Mezger, L.: Quaternary marine terraces, south-central coastal California: implications for crustal deformation and coastal evolution, in: *Quaternary coasts of the United States*, edited by: Fletcher, C.H., Wehmler, J.F., 323–332, <https://doi.org/10.2110/pec.92.48.0323>, 1992.
- 350 Harmon, R.S., Mitterer, R.M., Kriausakul, N., Land, L.S., Schwarcz, H.P., Garrett, P., Larson, G.J., Leonard Vacher, H., and Rowe, M.: U-series and amino-acid racemization geochronology of Bermuda:

- Implications for eustatic sea-level fluctuation over the past 250,000 years, *Palaeogeography, Palaeoclimatology, Palaeoecology*, 44, 41–70, [https://doi.org/10.1016/0031-0182\(83\)90004-4](https://doi.org/10.1016/0031-0182(83)90004-4), 1983.
- 355 Harrison, J. V.: Coastal Makran: Discussion, *The Geographical Journal*, 97, 15, <https://doi.org/10.2307/1787108>, 1941.
- Hays, J.D., Imbrie, J., Shackleton, N.J.: Variations in the earth's orbit: Pacemaker of the ice ages, *Science*, 1976.
- 360 Hearty, P.J.: The geology of Eleuthera Island, Bahamas: A Rosetta Stone of quaternary stratigraphy and sea-level history, *Quaternary Sci Rev*, 17, 333–355, [https://doi.org/10.1016/S0277-3791\(98\)00046-8](https://doi.org/10.1016/S0277-3791(98)00046-8), 1998.
- Hearty, P.J.: Revision of the late Pleistocene stratigraphy of Bermuda, *Sediment Geol*, 153, 1–21, [https://doi.org/10.1016/S0037-0738\(02\)00261-0](https://doi.org/10.1016/S0037-0738(02)00261-0), 2002
- 365 Hearty, P.J. and Kaufman, D.S.: Whole-rock aminostratigraphy and Quaternary sea-level history of the Bahamas, *Quaternary Res*, 54, 163–173, <https://doi.org/10.1006/qres.2000.2164>, 2000.
- Hearty, P.J., Vacher, H.L., and Mitterer, R.M.: Aminostratigraphy and ages of Pleistocene limestones of Bermuda, *Geol Soc Am Bull*, 104, 471–480, [https://doi.org/10.1130/0016-7606\(1992\)104<0471:AAAOPL>2.3.CO;2](https://doi.org/10.1130/0016-7606(1992)104<0471:AAAOPL>2.3.CO;2), 1992
- 370 Hertlein, L.G. and Grant IV, U.S.: The Geology and Paleontology of the Marine Pliocene of San Diego, California, *Memoirs of the San Diego Society of Natural History*, 2, 15-20, 1944
- [Hijma, M.P., Engelhart, S.E., Törnqvist, T.E., Horton, B.P., Hu, P., Hill, D.F.: A protocol for a geological sea-level database, in: Handbook of Sea-Level Research, edited by: Shennan, I., Long, A.J., Horton, B.P., 536-556, Germany, Wiley, 2015.](#)
- 375 [Hunter, J.D.: Matplotlib: A 2D Graphics Environment, Comput Sci Eng, 9, 3, 90-95, https://doi.org/10.1109/MCSE.2007.55, 2007.](#)
- [Huntley, D.J. and Prescott, J.R.: Improved methodology and new thermoluminescence ages for the dune sequence in south-east South Australia. Quaternary Sci Rev, 20, 687–699, 2001.](#)
- [Huntley, D.J., Hutton, J.T., Prescott, J.R.: The stranded beach-dune sequence of south-east South Australia: A test of thermoluminescence dating, 0-800 ka. Quaternary Sci Rev, 12, 1–20, 1993a.](#)
- 380 [Huntley, D.J., Hutton, J.T., Prescott, J.R.: Optical dating using inclusions within quartz grains. Geology, 21, 1087–1090, 1993b.](#)
- [Huntley D.J., Hutton J.T., Prescott J.R.: Further thermoluminescence dates from the dune sequence in southeast of South Australia, Quaternary Sci Rev, 13, 201–207, https://doi.org/10.1016/0277-3791\(94\)90025-6, 1994.](#)
- 385 Johnson, D.L.: Beachrock (water-table rock) on San Miguel Island, in: *Geology of the Northern Channel Islands*, edited by: Weaver, D.W., AAPG and SEPM Pacific, 1969.
- [Kelsey, H.M. and Bockheim, J.G.: Coastal landscape evolution as a function of eustasy and surface uplift rate, Cascadia margin, southern Oregon, Bull Geol Soc Am, 106, 840–854, https://doi.org/10.1130/0016-7606\(1994\)106<0840:CLEAAF>2.3.CO;2, 1994.](#)
- 390 Kelsey, H.M., Ticknor, R.L., Bockheim, J.G., and Mitchell, C.E.: Quaternary upper plate deformation in coastal Oregon, *Bull Geol Soc Am*, 108, 843–860, [https://doi.org/10.1130/0016-7606\(1996\)108<0843:QUPDIC>2.3.CO;2](https://doi.org/10.1130/0016-7606(1996)108<0843:QUPDIC>2.3.CO;2), 1996.

Deleted: .

Moved down [1]: J. D.

Deleted:

Moved (insertion) [1]

Deleted:

Deleted: "

Deleted: "

Deleted: in

Formatted: Font: Not Italic

Deleted: ing

Deleted: in

Deleted: ence

Deleted: &

Deleted: incering

Deleted: .

Deleted: .

- Kennedy, G.L., Lajoie, K.R., and Wehmiller, J.F.: Aminostratigraphy and faunal correlations of late Quaternary marine terraces, Pacific Coast, USA, *Nature*, 299, 545–547, <https://doi.org/10.1038/299545a0>, 1982.
- 410 Kennedy, G.L., Wehmiller, J.F., and Rockwell, T.K.: Paleoecology and paleozoogeography of late Pleistocene marine- terrace faunas of southwestern Santa Barbara County, California, in: *Quaternary coasts of the United States*, edited by: Fletcher, C.H., Wehmiller, J.F., 343–361, <https://doi.org/10.2110/pec.92.48.0343>, 1992.
- 415 Kern, J.P.: Late Quaternary deformation of the Nestor terrace on the east side of Point Loma, San Diego, California, in: *Studies on the geology and geologic hazards of the greater San Diego area, California*, edited by: Ross, A., and Dowlen, R. J., San Diego Assoc. Geologists and Assoc. Engineering, 1973.
- Kern, J. P.: Origin and history of upper Pleistocene marine terraces, San Diego, California, *Bull Geol Soc Am*, 88, 1553–1566, [https://doi.org/10.1130/0016-7606\(1977\)88<1553:OAHOUUP>2.0.CO;2](https://doi.org/10.1130/0016-7606(1977)88<1553:OAHOUUP>2.0.CO;2), 1977.
- 420 Kern, J.P. and Rockwell, T.K.: Chronology and deformation of Quaternary marine shorelines, San Diego County, California, in: *Quaternary coasts of the United States*, edited by: Fletcher, C.H., Wehmiller, J.F., 377–382, <https://doi.org/10.2110/pec.92.48.0377>, 1992.
- Kindler, P. and Hearty, P.J.: Carbonate petrography as an indicator of climate and sea-level changes: New data from Bahamian Quaternary units, *Sedimentology*, 43, 381–399, <https://doi.org/10.1046/j.1365-3091.1996.d01-11.x>, 1996.
- 425 Kopp, R.E., Simons, F.J., Mitrovica, J.X., Maloof, A.C., Oppenheimer, M.: Probabilistic assessment of sea level during the last interglacial stage, *Nature*, 462, 863–867, <https://doi.org/10.1038/nature08686>, 2009.
- 430 Ku, T.L. and Kern, J.P.: Uranium-series age of the upper pleistocene Nestor Terrace, San Diego, California, *Bull Geol Soc Am*, 85, 1713–1716, [https://doi.org/10.1130/0016-7606\(1974\)85<1713:UAOTUP>2.0.CO;2](https://doi.org/10.1130/0016-7606(1974)85<1713:UAOTUP>2.0.CO;2), 1974.
- Lambeck, K. and Chappell, J.: Sea level change through the last glacial cycle, *Science*, 292, 679–686, <https://doi.org/10.1126/science.1059549>, 2001.
- 435 Land, L. S., MacKenzie, F. T. and Gould, S. J.: Pleistocene history of Bermuda, *Geol. Soc. Am. Bull.*, 78, 993–1006, [https://doi.org/10.1130/0016-7606\(1967\)78\[993:PHOB\]2.0.CO;2](https://doi.org/10.1130/0016-7606(1967)78[993:PHOB]2.0.CO;2), 1967.
- [Latychev, K., Mitrovica, J.X., Tromp, J., Tamisiea, M.E., Komatitsch, D., Christara, C.C.: Glacial isostatic adjustment on 3-D earth models: A finite-volume formulation. \*Geophys J Int\* 161, 421–444, 2005.](#)
- 440 Lidz, B.H., Hine, A.C., Shinn, E.A., and Kindinger, J.L.: Multiple outer-reef tracts along the south Florida bank margin: outlier reefs, a new windward-margin model, *Geology*, 19, 115–118, [https://doi.org/10.1130/0091-7613\(1991\)019<0115:MORTAT>2.3.CO;2](https://doi.org/10.1130/0091-7613(1991)019<0115:MORTAT>2.3.CO;2), 1991.
- Lindgren, W.: Notes on the geology of Baja California, Mexico, *Proceedings of the California Academy of Sciences*, 1, 173–196, 1889.
- 445 [Lorscheid, T. and Rovere, A.: The indicative meaning calculator – quantification of paleo sea-level relationships by using global wave and tide datasets, \*Open Geospatial Data, Software and Standards\*, 4, 2019.](#)

Deleted: .

Deleted: .

Formatted: English (US)

Deleted: .

Formatted: English (US)

- 450 Ludwig, K.R., Muhs, D.R., Simmons, K.R., Halley, R.B., and Shinn, E.A.: Sea-level records at ~80 ka from tectonically stable platforms: Florida and Bermuda, *Geology*, 24, 211–214, [https://doi.org/10.1130/0091-7613\(1996\)024<0211:SLRAKF>2.3.CO;2](https://doi.org/10.1130/0091-7613(1996)024<0211:SLRAKF>2.3.CO;2), 1996.
- Marquardt, C., Lavenu, A., Ortlieb, L., Godoy, E., and Comte, D.: Coastal neotectonics in Southern Central Andes: Uplift and deformation of marine terraces in Northern Chile (27°S), *Tectonophysics*, 394, 193–219, <https://doi.org/10.1016/j.tecto.2004.07.059>, 2004.
- 455 **Matthews, R.K.: Relative elevation of late Pleistocene high sea level stands: Barbados uplift rates and their implications, *Quaternary Res.* 3, 147-153, [https://doi.org/10.1016/0033-5894\(73\)90061-6](https://doi.org/10.1016/0033-5894(73)90061-6), 1973.**
- McInelly, G.W. and Kelsey, H.M.: Late Quaternary tectonic deformation in the Cape Arago-Bandon region of coastal Oregon as deduced from wave-cut platforms, *J Geophys Res*, 95, 6699–6713, <https://doi.org/10.1029/JB095iB05p06699>, 1990.
- 460 Merritts, D. and Bull, W.B.: Interpreting Quaternary uplift rates at the Mendocino triple junction, northern California, from uplifted marine terraces, *Geology*, 17, 1020–1024, [https://doi.org/10.1130/0091-7613\(1989\)017<1020:IQRAT>2.3.CO;2](https://doi.org/10.1130/0091-7613(1989)017<1020:IQRAT>2.3.CO;2), 1989.
- Mesolella, K. J.: Zonation of Uplifted Pleistocene Coral Reefs on Barbados, West Indies, *Science*, 156, 638–640, 1967.
- 465 Mesolella, K.J., Matthews, R.K., Broecker, W.S., and Thurber, D.L.: The astronomical theory of climatic change: Barbados Data, *J Geol*, 77, 250–274, <https://doi.org/10.1086/627434>, 1969.
- Milankovitch, M.: Die chronologie des Pleistocens, *Bull Acad Sci Math Nat Belgr*, 4, 49, 1938.
- Miller, G.H., Hollin, J.T., Andrews, J.T.: Aminostratigraphy of UK Pleistocene deposits, *Nature*, 281, 539–543, <https://doi.org/10.1038/281539a0>, 1979.
- 470 Mirecki, J.E., Wehmiller, J.F., and Skinner, A.F.: Geochronology of Quaternary Coastal Plain Deposits, Southeastern Virginia, U.S.A., *J Coastal Res*, 11, 1135–1144, 1995.
- Mitterer, R.M.: Pleistocene stratigraphy in Southern Florida based on amino acid diagenesis in fossil mercuraria, *Geology*, 2, 425–428, [https://doi.org/10.1130/0091-7613\(1974\)2<425:PSISFB>2.0.CO;2](https://doi.org/10.1130/0091-7613(1974)2<425:PSISFB>2.0.CO;2), 1974.
- 475 Mueller, K., Kier, G., Rockwell, T., Jones, C.H.: Quaternary rift flank uplift of the Peninsular Ranges in Baja and southern California by removal of mantle lithosphere, *Tectonics*, 28, 1–17, <https://doi.org/10.1029/2007TC002227>, 2009.
- Muhs, D.R., Kelsey, H.M., Miller, G.H., Kennedy, G.L., Whelan, J.F., Mcinelly, G.W.: Age Estimates and Uplift Rates for Late Pleistocene Marine Terraces, *J Geophys Res*, 95, 6685–6698, <https://doi.org/10.1029/JB095iB05p06685>, 1990.
- 480 Muhs, D.R., Miller, G.H., Whelan, J.F., and Kennedy, G.L.: Aminostratigraphy and oxygen isotope stratigraphy of marine-terrace deposits, Palos Verdes Hills and San Pedro areas, Los Angeles County, California, in: *Quaternary coasts of the United States*, edited by: Fletcher, C.H., Wehmiller, 363–376, 1992a.
- 485 Muhs, D.R., Rockwell, T.K., Kennedy, G.L.: Late quaternary uplift rates of marine terraces on the Pacific coast of North America, southern Oregon to Baja California sur, *Quatern Int*, 15–16, 121–133, [https://doi.org/10.1016/1040-6182\(92\)90041-Y](https://doi.org/10.1016/1040-6182(92)90041-Y), 1992b.
- 490 Muhs, D.R., Kennedy, G.L., Rockwell, T.K.: Uranium-series ages of marine terrace corals from the Pacific coast of North America and implications for last-interglacial sea level history, *Quaternary Res*, 42, 72–87, <https://doi.org/10.1006/qres.1994.1055>, 1994.

Formatted: English (US)

- Muhs, D.R., Simmons, K.R., and Steinke, B.: Timing and warmth of the Last Interglacial period: New U-series evidence from Hawaii and Bermuda and a new fossil compilation for North America, *Quaternary Sci Rev*, 21, 1355–1383, [https://doi.org/10.1016/S0277-3791\(01\)00114-7](https://doi.org/10.1016/S0277-3791(01)00114-7), 2002.
- 495 Muhs, D.R., Simmons, K.R., Kennedy, G.L., Ludwig, K.R., and Groves, L.T.: A cool eastern Pacific Ocean at the close of the Last Interglacial complex, *Quaternary Sci Rev*, 25, 235–262, <https://doi.org/10.1016/j.quascirev.2005.03.014>, 2006.
- Muhs, D.R., Simmons, K.R., Schumann, R.R., Groves, L.T., Mitrovica, J.X., and Laurel, D.A.: Sea-level history during the Last Interglacial complex on San Nicolas Island, California: Implications for glacial isostatic adjustment processes, paleozoogeography and tectonics, *Quaternary Sci Rev*, 37, 1–25, <https://doi.org/10.1016/j.quascirev.2012.01.010>, 2012.
- 500 Muhs, D.R., Simmons, K.R., Schumann, R.R., Groves, L.T., DeVogel, S.B., Minor, S.A., and Laurel, D.A.: Coastal tectonics on the eastern margin of the Pacific Rim: Late Quaternary sea-level history and uplift rates, Channel Islands National Park, California, USA, *Quaternary Sci Rev*, 105, 209–238, <https://doi.org/10.1016/j.quascirev.2014.09.017>, 2014.
- 505 Murray-Wallace, C. V.: Pleistocene coastal stratigraphy, sea-level highstands and neotectonism of the southern Australian passive continental margin - A review, *J Quaternary Sci*, 17, 469–489, <https://doi.org/10.1002/jqs.717>, 2002.
- 510 [Murray-Wallace, C. V.: Quaternary history of the Coorong Coastal Plain, Southern Australia: An archive of environmental and global sea-level changes. Springer, Cham, 229, 2018.](#)
- Neumann, A.C. and Moore, W.S.: Sea level events and Pleistocene coral ages in the northern Bahamas, *Quaternary Res*, 5, 215–224, [https://doi.org/10.1016/0033-5894\(75\)90024-1](https://doi.org/10.1016/0033-5894(75)90024-1), 1975.
- Newell, N.D.: Warm interstadial interval in Wisconsin stage of the Pleistocene, *Science*, 148, 1488, <https://doi.org/10.1126/science.148.3676.1488>, 1965.
- 515 Normand, R., Simpson, G., Herman, F., Haque Biswas, R., Bahroudi, A., and Schneider, B.: Dating and morpho-stratigraphy of uplifted marine terraces in the Makran subduction zone (Iran), *Earth Surf Dynam*, 7, 321–344, <https://doi.org/10.5194/esurf-7-321-2019>, 2019
- Omura, A.: Uranium-series Age of the Riukiu Limestone on Hateruma Island, Southwestern Ryukyus, *Transactions and Proceedings of the Palaeontological Society of Japan*, 415–426, [https://doi.org/10.14825/prpsj1951.1984.135\\_415](https://doi.org/10.14825/prpsj1951.1984.135_415), 1984.
- 520 Omura, A., Maeda, Y., Kawana, T., Siringan, F.P., and Berdin, R.D.: U-series dates of Pleistocene corals and their implications to the paleo-sea levels and the vertical displacement in the Central Philippines, *Quatern Int*, 115–116, 3–13, [https://doi.org/10.1016/S1040-6182\(03\)00092-2](https://doi.org/10.1016/S1040-6182(03)00092-2), 2004.
- 525 Orr, P.C.: Prehistory of Santa Rosa Island, Santa Barbara Museum of Natural History, Santa Barbara, California, 1968.
- Osmond, J.K., Carpenter, J.R., Windom, H.L.: Th 230 /U 234 age of the Pleistocene corals and oolites of Florida, *J Geophys Res*, 70, 1843–1847, <https://doi.org/10.1029/JZ070i008p01843>, 1965.
- Ota, Y. and Hori, N.: Late Quaternary tectonic movement of the Ryukyu Islands, Japan, *The Quaternary Research (Daiyonki-kenkyu)*, 18, 221–240, <https://doi.org/10.4116/jaqua.18.221>, 1980.
- 530 Ota, Y. and Omura, A.: Contrasting styles and rates of tectonic uplift of coral reef terraces in the Ryukyu and Daito Islands, southwestern Japan, *Quatern Int*, 15–16, 17–29, [https://doi.org/10.1016/1040-6182\(92\)90033-X](https://doi.org/10.1016/1040-6182(92)90033-X), 1992.

Formatted: English (US)

- Page, W. D., Alt, J. N., Cluff, L. S., and Plafker, G.: Evidence for the recurrence of large-magnitude earthquake along the Makran coast of Iran and Pakistan, *Tectonophysics*, 52, 533–547, [https://doi.org/10.1016/0040-1951\(79\)90269-5](https://doi.org/10.1016/0040-1951(79)90269-5), 1979.
- 535 Parham, P.R., Riggs, S.R., Culver, S.J., Mallinson, D.J., Jack Rink, W., and Burdette, K.: Quaternary coastal lithofacies, sequence development and stratigraphy in a passive margin setting, North Carolina and Virginia, USA, *Sedimentology*, 60, 503–547, <https://doi.org/10.1111/j.1365-3091.2012.01349.x>, 2013.
- 540 Perg, L.A., Anderson, R.S., Finkel, R.C.: Use of a new  $^{10}\text{Be}$  and  $^{26}\text{Al}$  inventory method to date marine terraces, Santa Cruz, California, USA, *Geology*, 29, 879–882, [https://doi.org/10.1130/0091-7613\(2001\)029<0879:UOANBA>2.0.CO;2](https://doi.org/10.1130/0091-7613(2001)029<0879:UOANBA>2.0.CO;2), 2001.
- Pinter, N., Johns, B., Little, B., and Vestal, W.D.: Fault-related folding in California’s Northern Channel Islands documented by rapid-static GPS positioning, *GSA Today*, 11, 4–9, [https://doi.org/10.1130/1052-5173\(2001\)011<0004:FRFICN>2.0.CO;2](https://doi.org/10.1130/1052-5173(2001)011<0004:FRFICN>2.0.CO;2), 2001.
- 545 Potter, E.K. and Lambeck, K.: Reconciliation of sea-level observations in the Western North Atlantic during the last glacial cycle, *Earth Planet Sc Lett*, 217, 171–181, [https://doi.org/10.1016/S0012-821X\(03\)00587-9](https://doi.org/10.1016/S0012-821X(03)00587-9), 2004.
- 550 Potter, E.K., Esat, T.M., Schellmann, G., Radtke, U., Lambeck, K., McCulloch, M.T.: Suborbital-period sea-level oscillations during marine isotope substages 5a and 5c, *Earth Planet Sc Lett*, 225, 191–204, <https://doi.org/10.1016/j.epsl.2004.05.034>, 2004.
- Railsback, L.B., Gibbard, P.L., Head, M.J., Voarintsoa, N.R.G., Toucanne, S.: An optimized scheme of lettered marine isotope substages for the last 1.0 million years, and the climatostratigraphic nature of isotope stages and substages, *Quaternary Sci Rev*, 111, 94–106, <https://doi.org/10.1016/j.quascirev.2015.01.012>, 2015.
- 555 Reyss, J.L., Pirazzoli, P.A., Haghypour, A., Hatté, C., and Fontugne, M.: Quaternary marine terraces and tectonic uplift rates on the south coast of Iran, *Geol Soc SP*, 146, 225–237, <https://doi.org/10.1144/GSL.SP.1999.146.01.13>, 1998.
- 560 Ringor, C.L., Omura, A., and Maeda, Y.: Last Interglacial Terraces Sea Level in Southwest Changes Deduced Central from Coral Reef Terraces in Southwest Bohol, Central Philippines, *The Quaternary Research*, 46, 401–416, <https://doi.org/10.4116/jaqua.43.401>, 2004.
- Rockwell, T.K., Muhs, D.R., Kennedy, G.L., Hatch, M.E., Wilson, S.H., and Klinger, R.E.: Uranium-Series Ages, Faunal Correlations and Tectonic Deformation of Marine Terraces Within the Agua Blanca Fault Zone at Punta Banda, Northern Baja California, Mexico, *Geologic Studies in Baja California*, 1–16, 1989.
- 565 Rockwell, T.K., Nolan, J., Johnson, D.L., and Patterson, R.H.: Age and Deformation of Marine Terraces Between Point Conception and Gaviota, Western Traverse Ranges, California, in: *Quaternary coasts of the United States*, edited by: Fletcher, C.H., Wehmiller, 333–341, 1992.
- 570 Rovere, A., Raymo, M.E., Vacchi, M., Lorscheid, T., Stocchi, P., Gómez-Pujol, L., Harris, D.L., Casella, E., O’Leary, M.J., Hearty, P.J.: The analysis of Last Interglacial (MIS 5e) relative sea-level indicators: Reconstructing sea-level in a warmer world, *Earth-Sci Rev*, 159, 404–427, <https://doi.org/10.1016/j.earscirev.2016.06.006>, 2016.

Deleted: .

Deleted: 3

- 575 Rovere, A., Ryan, D., Murray-Wallace, C., Simms, A., Vacchi, M., Dutton, A., ... Gowan, E.: Descriptions of database fields for the World Atlas of Last Interglacial Shorelines (WALIS) (Version 1,0), Zenodo, <http://doi.org/10.5281/zenodo.3961544>, 2020.
- 580 Schellmann, G., Radtke, U.: A revised morpho- and chronostratigraphy of the Late and Middle Pleistocene coral reef terraces on Southern Barbados (West Indies), *Earth-Sci Rev.* 64, 157–187, 2004.
- Schwebel, D.A.: Quaternary Stratigraphy and Sea-Level Variation in the Southeast of South Australia, in: Coastal Geomorphology in Australia, edited by: Thom, B.G., Academic Press, Sydney, 291 – 311.
- Sherman, C.E., Fletcher, C.H., Rubin, K.H., Simmons, K.R., Adey, W.H.: Sea-level and reef accretion history of Marine Oxygen Isotope Stage 7 and late Stage 5 based on age and facies of submerged late Pleistocene reefs, Oahu, Hawaii, *Quaternary Res.* 81, 138–
- 585 150, <http://dx.doi.org/10.1016/j.yqres.2013.11.001>, 2014.
- Simms, A.R., DeWitt, R., Rodriguez, A.B., Lambeck, K., Anderson, J.B.: Revisiting marine isotope stage 3 and 5a (MIS3-5a) sea levels within the northwestern Gulf of Mexico, *Global Planet Change*, 66, 100–111, <https://doi.org/10.1016/j.gloplacha.2008.03.014>, 2009.
- Simms, A.R., Rouby, H., and Lambeck, K.: Marine terraces and rates of vertical tectonic motion: The importance of glacio-isostatic adjustment along the Pacific coast of central North America, *Bull Geol Soc Am*, 128, 81–93, <https://doi.org/10.1130/B31299.1>, 2016.
- 590 Sprigg, R.C.: Stranded Pleistocene sea beaches of South Australia and aspects of the theories of Milankovitch and Zeuner, *Int. Geol. Congr.(XVI. II, GB, 1948)*, 1952.
- Szabo, B.J.: Uranium-series dating of fossil corals from marine sediments of southeastern United States Atlantic Coastal Plain, *Geol Soc Am Bull*, 96, 398–406, [https://doi.org/10.1130/0016-7606\(1985\)96<398:UDOFCE>2.0.CO;2](https://doi.org/10.1130/0016-7606(1985)96<398:UDOFCE>2.0.CO;2), 1985.
- 595 Szabo, B.J. and Rosholt, J.N.: Uranium-series dating of Pleistocene molluscan shells from southern California-An open system model, *J Geophys Res*, 74, 3253–3260, <https://doi.org/10.1029/jb074i012p03253>, 1969.
- 600 Thompson, S., and Creveling, J.R.: WALIS Spreadsheet Thompson Creveling, Zenodo, <https://doi.org/10.5281/zenodo.4426206>, 2021
- Thurber, D.L., Broecker, W.S., Blanchard, R.L., Potratz, H.A.: Uranium-series ages of Pacific atoll coral, *Science* 149, 55–58, 1965.
- Toscano, M.A. and Lundberg, J.: Submerged late pleistocene reefs on the tectonically-stable S.E. Florida margin: High-precision geochronology, stratigraphy, resolution of substage 5a sea-level elevation, and orbital forcing, *Quaternary Sci Rev*, 18, 753–767, [https://doi.org/10.1016/S0277-3791\(98\)00077-8](https://doi.org/10.1016/S0277-3791(98)00077-8), 1999.
- 605 Vacchi, M., Montefalcone, M., Schiaffino, C.F., Parravicini, V., Bianchi, C.N., Morri, C., Ferrari, M.: Towards a predictive model to assess the natural position of the *Posidonia oceanica* seagrass meadows upper limit, *Mar Pollut Bull.* 83, 458–466, 2014.
- 610 Vacher, H.L. and Hearty, P.: History of stage 5 sea level in Bermuda: Review with new evidence of a brief rise to present sea level during Substage 5a, *Quaternary Sci Rev*, 8, 159–168, [https://doi.org/10.1016/0277-3791\(89\)90004-8](https://doi.org/10.1016/0277-3791(89)90004-8), 1989
- Valensise, G., and Ward, S.N.: Long-term uplift of the Santa Cruz coastline in response to repeated earthquakes along the San Andreas Fault, *B Seismol Soc Am*, 81, 1694–1704, 1991.

Deleted :

- Vedder, J.G. and Norris, R.M.: Geology of San Nicolas Island California, US Geological Survey Professional Paper, 369, 65 pp, 1963
- 620 Vedder, J. G., Yerkes, R. F., and Schoelhamer, J. E.: Geologic map of the San Joaquin Hills– San Juan Capistrano area, Orange County, California, U.S. Geological Survey Oil and Gas Investigations, 1957.
- Veeh, H.H., and Chappell, J.: Astronomical Theory of Climatic Change, Support from New Guinea, Science, 167, 862–865, <https://doi.org/10.1126/science.167.3919.862>, 1970.
- 625 Wehmiller, J.F., Simmons, K.R., Cheng, H., Edwards, R.L., Martin-McNaughton, J., York, L.L., Krantz, D.E., and Shen, C.C.: Uranium-series coral ages from the US Atlantic Coastal Plain-the “80 ka problem” revisited, Quatern Int, 120, 3–14, <https://doi.org/10.1016/j.quaint.2004.01.002>, 2004.
- [Wehmiller, J.F., Brothers, L.L., Ramsey, K.W., Foster, D.S., Mattheus, C.R.: Molluscan aminostratigraphy of the US Mid-Atlantic Quaternary coastal system: implications for onshore-offshore correlation, paleochannel and barrier island evolution, and local late Quaternary sea-level history, Quat Geochronol, 2021a.](#)
- 630 [Wehmiller, J.F., May 2<sup>nd</sup>, Summary of Amino Acid Racemization data and associated geochronological data, US Atlantic Coastal Plain, <https://arcg.is/1L0uyK>, 2021b.](#)
- Woodring, W.P., Brown, J.S., Burbank, W.S.: Geology of the Republic of Haiti, Lord Baltimore Press, 631 p, 1924.
- 635 Woodring, W. P., Bramlette, M. N., Kew, W. S. W.: Geology and Paleontology of Palos Verdes Hills, California, U.S. Government Printing Office, 145, 1946.

Formatted: Superscript

Deleted: , 2021b

Formatted: English (US)



Page 20: [1] Deleted Thompson, Schmitt Blue 6/3/21 10:27:00 AM

Page 26: [2] Deleted Jessica Creveling 6/4/21 4:37:00 PM

Page 26: [3] Deleted Thompson, Schmitt Blue 4/2/21 3:30:00 PM

Page 26: [4] Deleted Jessica Creveling 6/4/21 4:37:00 PM